Scilight

Habitable Planet, 2026, 2(2), 448–467

Habitable Planet

Journal Homepage: https://www.sciltp.com/journals/hp

Review

Terrestrial Ecological Disturbances and Responses to Palaeowildfires at the Permian–Triassic Transition, A Review of Current Research

Longyi Shao[1,*], Fanghui Hua[1,2,*], Timothy P. Jones[3], Tianchang Zhang[1], Xuetian Wang[1], Zhiming Yan[4], Jing Lu[1], and Jason Hilton[5]

[1] College of Geoscience and Surveying Engineering, China University of Mining and Technology, Beijing 100083, China
[2] Hebei Institute of Geological Survey, Shijiazhuang 050200, Hebei Province, China
[3] School of Earth and Environmental Sciences, Cardiff University, Cardiff CF10 3YE, Wales, UK
[4] Institute of Architectural Engineering, Weifang University, Weifang 261061, Shandong Province, China
[5] Geography, Earth and Environmental Sciences, University of Birmingham, Birmingham B15 2TT, UK
[*] Correspondence: ShaoL@cumtb.edu.cn (L.S.); Huafh9312@163.com (F.H.)

ABSTRACT

At the end of the Paleozoic Era, the Earth experienced an extreme ecosystem disturbance event, which was the Permian–Triassic Mass Extinction (PTME); causing an irreversible global catastrophe for animals and plants. Fossil evidence from marine strata correlated by zircon U–Pb dating of volcanic ash supports the view of a rapid and short-lived extinction. In contrast, the associated disturbance processes of terrestrial ecosystems were relatively prolonged and complex, leading different scholars to propose various extinction mechanisms and models for these ecosystem disturbances. Evidence of wildfires in late Permian–Early Triassic transitional strata have been reported globally, and many scholars believe that wildfires during the PTME were a significant contributing factor to terrestrial ecosystem disturbance. Globally, palaeowildfires may have served as an important driver for terrestrial ecosystem disturbance during the Permian–Triassic transition, promoting and accelerating the processes of environmental degradation. Palaeowildfires during the Permian–Triassic transition played a crucial role in the changing of terrestrial ecosystems with potential implications for the evolution of larger ecosystems. This study systematically reviews progress in recent research on the terrestrial PTME and wildfires. It summarizes and considers the mechanisms of terrestrial ecosystem disturbance during the P–T transition and responses to palaeowildfires, considering the palaeoenvironmental background and plant evolution processes.

ARTICLE INFO

History:

Received: 06 July 2026
Revised: 12 August 2026
Accepted: 21 August 2026
Published: 09 September 2026

Keywords:

Permian–Triassic Mass Extinction (PTME);
terrestrial ecological disturbance;
floral change;
palaeowildfire

Citation:

Shao, L.; Hua, F.; Jones, T.P.; et al. Terrestrial Ecological Disturbances and Responses to Palaeowildfires at the Permian–Triassic Transition, A Review of Current Research. *Habitable Planet* **2026**, *2*(2), 448–467. https://doi.org/10.63335/j.hp.2026.0048

Copyright: © 2026 by the authors. This is an open access article under the terms and conditions of the Creative Commons Attribution (CC BY) license (https://creativecommons.org/licenses/by/4.0/).
Publisher's Note: Scilight stays neutral with regard to jurisdictional claims in published maps and institutional affiliations.

Research Highlights

- Multi-stage and long-duration terrestrial ecological disturbance during the Permian–Triassic transition.
- Wildfire played an important role in the terrestrial mass extinction.
- Wildfires destroyed vegetation but were also an agent for renewal and change.

1. Introduction

Today, large-scale anthropogenic ecological habitat destruction and pollution have severely threatened biodiversity and the sustainability of many of the Earth's ecosystems [1]. A growing number of researchers believe that the Earth is currently experiencing a sixth mass extinction event [1]. Deep time palaeoclimatology is a hot topic in current sedimentology research. Major climate change events in geological history can serve as ecological analogs for the future evolution of the Earth's environment, providing insights and guidance for human development [2]. The end of the late Paleozoic was a critical turning point in the ecological-environmental evolution of geological history, during which the largest biological crisis of the Phanerozoic occurred—the Permian–Triassic mass extinction (PTME) [3, 4]. Following the PTME, a global "coal gap" occurred in the Early Triassic, and terrestrial ecosystems did not significantly recover until approximately 10 million years [5, 6]. Although extensive research has been conducted on this major extinction event, opinions remain divided, with various extinction processes and mechanisms proposed. The most generally accepted explanation is that large-scale volcanic activity at the Permian–Triassic boundary led to the gradual disturbance of global ecosystems [7–9]. Significant progress has been made in understanding marine extinctions, with high-precision volcanic ash dating constraining the main pulse duration of the extinction to 31 $\pm$ 31 kyr [10]. However, due to the influence of sedimentary facies variations, terrestrial strata are more complex, and correlations of contemporaneous strata often remain controversial [11]. In recent years, high-precision zircon U–Pb dating of volcanic ash in terrestrial strata has been widely reported [12–15], yet the timing of the onset of terrestrial biotic extinction across different latitudinal zones remains poorly resolved.

Although this phenomenon is attributed to ecological stress differences formed by latitudinal gradients, the underlying reasons still require further investigation. Firstly, terrestrial ecological disturbance does not usually equate to immediate collapse; rather, ecosystems collapse suddenly only when a series of environmental deteriorations exceed the self-regulatory or recovery capacity of the ecosystem [16]. Additionally, negative shifts in organic carbon isotopes and mercury enrichment events in the strata indicate a modest correspondence between terrestrial ecosystem disturbance and the marine biotic extinction [17, 18]. However, the extinction process of terrestrial plants may not be as brief and synchronous as that of marine organisms [13, 19, 20]. Dating indicates that terrestrial ecological disturbances occurred 60–370 kyr earlier than marine ecological disturbances [21] and exhibited distinct regional and phased characteristics [22–25]. Therefore, in-depth research into the gradual disturbance process of the Earth's ecosystem prior to the extinction and the associated palaeoenvironmental conditions are key to revealing the patterns and mechanisms of the PTME.

Forest fires (wildfires) have been widespread over both modern and geological history, imposing significant ecological pressure indirectly on marine and directly on terrestrial systems [26]. Large-scale wildfires threaten the stability of terrestrial ecosystems, disrupt hydrological cycles, and can even lead to a decline in regional species diversity [27, 28]. Wildfire events during the PTME have been widely reported and are considered an important factor in the terrestrial ecosystem crisis [29–31]. As a common natural phenomenon, wildfires are typically ignited by lightning and play an important role in many of the Earth's ecosystems [32]. On a global scale, wildfires produce large amounts of greenhouse gases, leading to global warming, and also generate harmful gases that threaten animal survival [33]. The behavior of animals and plants can influence the occurrence of wildfires by regulating the quantity, type, and condition of wildfire fuels, thus indicating an interaction between wildfires and the evolution of animals and plants [26, 34]. Coal is not only an important energy resource but also a significant carrier of deep time palaeoenvironmental information. The organic macerals in coal and sedimentary rocks record the evolution of the coal-forming environments and plant communities, while also preserving key information about palaeowildfires [35]. Inertinite is an important maceral group in coal and often can be found in other sediments. Due to its widely accepted origin from charring, inertinite can serve as evidence of palaeowildfires, and its reflectance can be used to infer combustion temperatures, thereby determining the type of wildfire [36]. In recent years, geological researchers have increasingly studied frequent palaeowildfire events during coal-forming periods, with these studies primarily using the content and distribution of inertinite as direct evidence of palaeowildfires [37–39]. Wildfire events during the PTME have been widely reported and are considered an important factor in the terrestrial ecosystem crisis [17, 31, 40, 41]. Frequent wildfires can directly kill plants and damage regional ecological environments, triggering a series of ecological and environmental issues [28]. Wildfires possess immense destructive power, capable of causing severe damage to local ecosystems in a short period [42]. Evidence of frequent palaeowildfires has been found globally in late Permian–Early Triassic transitional strata, suggesting that intense palaeowildfires may have played a significant role during the P–T terrestrial ecosystem disturbance [31, 40, 43]. In recent years, forest fires have shown a global trend of increasing occurrence and severity [44], threatening the stability of local ecosystems. Although some scholars still argue that forest fires are a means of natural ecological self-regulation and cannot cause entire ecosystem disturbance [29], frequent wildfires globally could evolve into disaster events for the entire Earth [45]. Wildfires may not solely cause mass extinction events, but they could be a critical factor in tipping the balance of already fragile ecosystems. Therefore, research on late Permian–Early Triassic palaeowildfire events can not only provide insights into the causes of terrestrial ecosystem disturbance during the PTME but also provide a deep-time analog for the evolution of modern ecosystems.

This paper reviews and discusses the processes of terrestrial ecosystem disturbance, vegetation evolution, and palaeowildfire events during the Permian–Triassic transition. The relationship between wildfires and the evolution of the Earth's ecosystem are considered, with the aim of providing ideas and directions for modern environmental research and deep-time palaeoenvironmental analysis.

2. Mass Extinction During the Permian–Triassic Transition

Since the Cambrian explosion the Earth has experienced multiple major mass extinction events [22, 46]. These events led to significant reductions in global biodiversity at those times, had a major impact on the entire Earth's ecosystems, and altered the course of biological evolution [47]. The Permian–Triassic mass extinction is considered the most severe extinction event in geological history, resulting in the extinction of over 90% of marine invertebrates and about 70% of terrestrial vertebrates. Terrestrial plants also suffered major losses [48]. During this extinction event, marine organisms such as corals, fusulinids, and echinoderms nearly vanished, with only a few genera surviving. Extinction rates for bivalves, brachiopods, crinoids, and other organisms exceeded 90% [49, 50]. Following the PTME, marine populations evolution became more static, and diversity plummeted to levels almost matching the pre-Cambrian. Terrestrial ecosystems were also severely impacted, with a sharp decline in terrestrial plant genera and species with an extinction rate over 70%, and a coal gap of nearly 10 million years occurred [25, 51]. It took millions of years for the Earth's environment to recover to a state suitable for the survival of most organisms [52].

In recent years, a series of breakthroughs have been made in research on the Permian–Triassic boundary, particularly through U–Pb isotopic geochronology of volcanic ash layers using CA-ID-TIMS technology. This work has refined the temporal framework of the late Permian–Early Triassic transition, constraining the timing of marine biotic extinction during the Permian–Triassic transition to a precise range [10, 14], and it is considered a sudden and brief catastrophic event on a global scale. In different sections, variations in fossil record statistics led to different interpretations of the extinction process. Using cyclostratigraphy at the Shangsi section in Sichuan, it was inferred that the marine extinctions might have lasted up to 700 kyr, spanning a stratigraphic thickness of about 4.6 m [53]. At the GSSP section in Meishan, Changxing, Zhejiang, the main pulse of extinction spans the conodont zones *Clarkina meishanensis* Zone to the *Isarcicella isarcica* Zone; lasting about 30 kyr years and corresponding to Beds 25–28 [54]. However, the extinction interval in the Meishan section is only 0.36 metres thick, representing a highly condensed segment that might obscure the record of the extinction process [55, 56]. Some analyses suggest that the PTME process might be divided into two phases, corresponding to Beds 25 and 28 at Meishan, separated by a 180 kyr recovery period [55]. Other scholars point to another major extinction event at Bed 34 in the Meishan section, 446 kyr years after the main extinction pulse [57]. Regardless of the specific interpretations, the mass extinction event occurred during the Permian to Triassic transition. The differences lie in the spatial and temporal variations in the extinction of biotas, which may be attributed to the varying degrees of adaptation of different species to environmental deterioration [16], while also not disregarding preservational variations and consistency in the sequences.

Due to temporal synchronicity, large-scale volcanism is considered the primary trigger for the series of environmental disturbances during the PTME [7, 9, 58]. Hg concentration anomalies, as an important indicator of volcanic activity, have also been widely discovered in Permian–Triassic transitional strata [59–61]. Shen et al. analyzed Hg concentrations in 10 marine sections in the Northern Hemisphere, finding peaks near the Permian–Triassic Boundary (PTB), indicating a coupling between biotic extinction and volcanic activity [60]. Furthermore, the tonstein in the top C1 coal of the Xuanwei Formation and the mudstone containing volcaniclastic material at the top of the Kayitou Formation in the southwestern region

[62, 63] all indicate frequent volcanic activity during the late Permian–Early Triassic. Recently, Zhang et al. found high enrichment of Cu and Hg in extinction horizons in south China, demonstrating frequent regional volcanic activity during the PTME, synchronous in time with the Siberian Traps large igneous province [10]. This suggested that the Siberian Traps might not be the sole trigger for the PTME, and felsic volcanic activity at the margin of the south China Block was another cause of the terrestrial ecosystem crisis [9].

Recent studies indicate that the Siberian Traps large igneous province itself, and particularly the intrusion of its magmas into the sediment-rich Tunguska Basin, released large amounts of greenhouse gases such as CO_2 and CH_4, leading to severe global greenhouse effects [64]. This rapid increase in global CO_2 levels is also reflected in the stomatal index of *Lepidopteris* plant fossil leaves from the Early Triassic [5]. Significant fluctuations in the global carbon cycle are considered a major factor causing the collapse of marine ecosystems. Existing research shows anomalies in numerous geochemical indicators at the end-Permian extinction level, among which carbon isotopes (δ^{13}C) represent fluctuations in the deep-time palaeoclimate carbon cycle [65]. Carbon isotopes in marine sections show a rapid negative shift of about 5‰ during the PTME, a negative excursion also observed in terrestrial sections [66]. Therefore, the carbon isotope negative shift is often used as a tool for correlation between marine and terrestrial records. However, due to the variability of terrestrial sedimentation, this correlation tool remains controversial, and the process of terrestrial ecosystem disturbance is not unified [17, 25].

In addition to the global negative shift in carbon isotopes (δ^{13}C) caused by carbon cycle fluctuations, sulfur isotopes (δ^{34}S) [67, 68], oxygen isotopes (δ^{18}O) [69, 70], and calcium isotopes (δ^{44}Ca) [71] all show significant anomalies during the Permian–Triassic Transition. These indicate phenomena such as acid rain, elevated seawater temperatures, ocean acidification, and marine anoxia, respectively. These ecological and environmental changes are all considered important factors in marine biotic extinction [72]. Large-scale volcanic activity, while releasing greenhouse gases, also is accompanied by the emission of large amounts of halogens (F, Cl, etc.) or heavy metal elements [73]. This not only caused short-term snowball effects and acid rain events [9] but also led to ozone layer depletion over the long term.

Depletion of the ozone layer results in elevated radiation levels, thereby impacting the survival of flora and fauna [22]. Recent studies have found evidence of increased radiation in plant spores and pollen at the end of the Permian [73]. Although heavy metal toxicity has been proposed as a driver by some studies, evidence from south Tibet implicates ozone layer disruption [74]. Simulation studies indicate that atmospheric CO_2 levels increased rapidly by sixfold during the PTME, leading to rapid global warming [75]. Due to the intensified greenhouse effect, seawater temperatures rose, and ocean acidification occurred simultaneously [76]. Coupled with increased terrestrial clastic input [23], marine anoxia events followed [77]. The occurrence of the PTME was likely not due to a single factor but rather the combined effect of multiple components, with frequent volcanic activity potentially being the main trigger for this mass extinction (Figure 1).

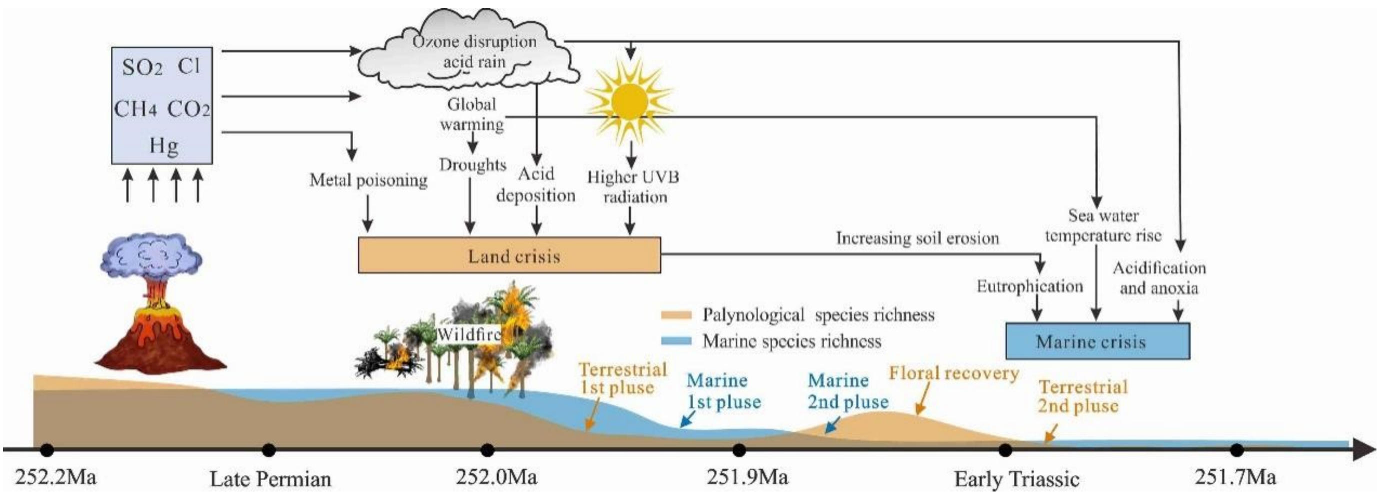

Figure 1. PTME ecological disturbance pattern. Marine species data and palynological data are from REFs [21, 25].

3. Terrestrial Ecosystem Disturbance during the P–T Transition

Research on the PTME began with marine strata, where statistics on marine biodiversity revealed the occurrence of the mass extinction event. Terrestrial strata are significantly influenced by palaeogeographic environments and are laterally variable, posing challenges for stratigraphic correlation and division [63]. Consequently, initial studies on the PTME in terrestrial strata did not yield a unified view. In recent years, with the increase in experimental techniques and research methods, reports of the PTME in terrestrial strata have become more frequent. The Karoo Basin in South Africa [78, 79], the Sydney Basin in Australia [80], and southwest China are areas with relatively well-studied late Permian–Early Triassic terrestrial strata [81]. Coupled with precise volcanic ash dating data, it has become possible to establish connections between terrestrial PTME events in different regions. The late Permian–Early Triassic terrestrial strata in the South African Karoo Basin preserve unique and well-preserved terrestrial animal assemblages (*Lystrosaurus*). The main extinction interval is considered to occur between the *Daptocephalus* and *Lystrosaurus declivis* assemblage zones [81], providing a basis for animal fossils from the PTME period. The latest research evidence finds that the decline in animal diversity in the Karoo Basin during the late Permian–Early Triassic transition occurred over a long duration of approximately 1 million years [79]. The late Permian strata of the Sydney Basin in Australia represents one of the few coal-bearing sequences, preserving a rich *Glossopteris* flora, and providing data on high-latitude plant diversity during the PTME. Recent research indicates that the extinction of the high-latitude *Glossopteris* flora occurred earlier than the marine extinction interval [13]. The Permian–Triassic transitional terrestrial strata in southwestern China preserve well-documented *Gigantopteris* flora fossils [24], providing a basis for studying the changes in low-latitude tropical flora. The latest zircon ages from volcanic ash layers indicate that the timing of the low-latitude terrestrial vegetation crisis occurred later than the marine extinction interval. We propose that this may be attributed to the lower ecological pressure in the low latitudes during the end-Permian, given the delayed arrival of extreme climates.

3.1. Carbon Cycle Perturbation and Volcanic Activity

A pronounced negative carbon isotope excursion is observed globally in strata near the Permian–Triassic Boundary (PTB). This is often attributed to the release of ^{12}C associated with the Siberian Traps Large Igneous Province [57, 82]. Fluctuations in the stable carbon isotope composition of organic matter ($\delta^{13}C_{org}$) typically reflect changes in atmospheric CO_2 composition [83, 84] and are linked to ecosystem disturbances during the PTME [85]. Several terrestrial sections in south China (Yantang, Fuyuan, Mide, Lengqinggou, and the Xuanwei H401 borehole core) show similar trends in $\delta^{13}C_{org}$ [17, 19, 43, 66]. A significant negative excursion occurs near the top of the Xuanwei Formation or the base of the Kayitou Formation, accompanied by changes in terrestrial flora and the appearance of fungal spikes, such as *Reduviasporonites* [22, 25, 86, 87]. The fungal peak has not been confirmed on a global scale, suggesting that it may not be inferred as a global fungal event.

The use of mercury (Hg) concentration anomalies in strata as an indicator of volcanic activity has been widely applied [59]. The synchroneity between the Siberian Traps Large Igneous Province and the PTME has been established, and has been considered the direct cause of the mass extinction and ecological environmental crisis [88], as well as the primary reason for Hg concentration anomalies near the PTB. Hg concentration peaks in ten marine sections across the Northern Hemisphere all occur near the PTB, and Hg isotope data indicate an atmospheric source for the Hg, further supporting the coupling between marine extinction and volcanic activity [89]. In Permian–Triassic transitional strata, peaks in Hg concentration show clear synchronicity with the negative carbon isotope excursion and species decline.

The negative carbon isotope excursion during the PTME has become one of the markers for stratigraphic correlation across different regions. In marine strata from this period, the negative δ^{13}C excursion coincides with Hg anomalies, reflecting contemporaneous climatic and environmental changes and serving as an important stratigraphic correlation tool [17, 21, 90]. Based on this, a preliminary link between marine and terrestrial strata has been established. As shown in Figure 2, unlike the single negative δ^{13}C excursion observed in marine carbonate strata, the negative $\delta^{13}C_{org}$ excursion in terrestrial strata often exhibits multiple phases, and Hg concentrations also show multiple peaks. These differences are often attributed to unreliable terrestrial stratigraphic correlation/division or tectonic influences on the strata. However, given the pervasiveness of this phenomenon, it is more likely that there are inherent differences between terrestrial ecosystem disturbance and marine biotic extinction. In other words, unlike the single, brief extinction process in marine strata, terrestrial ecosystem disturbance was likely a longer-term, multi-phase process.

The Siberian Traps Large Igneous Province is widely accepted as the primary cause of the PTME, but its duration far exceeds the constrained marine extinction interval [88]. Previous research indicates that the Siberian Traps began erupting in the early late Permian. The phase of sharp marine biodiversity decline corresponds to the intrusive stage of the Siberian Traps, and the large igneous province continued erupting after the mass extinction [7]. Recent studies on atmospheric CO_2 concentration changes during the PTME reveal a two-phase increase in the rate of CO_2 rise, with different sources for each phase. The first phase involved CO_2 from a slower-emission combustion-related heat source, while the second phase involved CO_2 from a faster-emission, mantle-dominated volcanic source [14, 91]. Therefore, the carbon cycle perturbation during the Permian–Triassic transition was multi-causal and multi-phase. Due to the directness and sensitivity of the terrestrial environment to atmospheric conditions, the chemical records in terrestrial strata may better reflect the changes in ecological environmental disturbance at that time.

3.2. Vegetation Evolution Processes

The extreme environments during the PTME event were equally devastating to marine animals and terrestrial plants [22, 92, 93]. The PTME ended the dominance of pteridophytes on land for over 200 million years, caused a global coal gap lasting millions of years [94], and marked a turning point in terrestrial plant evolution from pteridophytes to gymnosperms. However, previous studies found that the reduction in plant genera and species appears to be a regional phenomenon, and vegetation in different regions may have responded to the PTME to varying degrees due to latitudinal gradients and ecological pressures [22, 95].

The variability of terrestrial strata makes obtaining continuous plant macrofossil records challenging, hindering high-resolution description of the terrestrial plant extinction process. Unlike scattered plant macrofossils, spore-pollen assemblages can provide continuous information on plant evolution [26]. The study of spore-pollen fossils is significant for reconstructing palaeovegetation succession and palaeoclimate evolution [96, 97]. Nevertheless, previous palynological investigations from multiple terrestrial sections have yielded contradictory interpretations regarding vegetation turnover during the PTME. One view suggests that the terrestrial plant extinction process during the PTME was sudden and brief, similar to the marine biotic extinction [98]. Another view suggests that plant evolution during the PTME was a gradual process without a major extinction event [24, 99]. These differing views might stem from influences like sedimentary hiatus or regional palaeogeography, or they may be unclear due to a lack of precise dating data [100, 101]. Therefore, to better study the evolution of terrestrial plant communities and determine the disturbance patterns of terrestrial ecosystems during the Permian–Triassic transition, stable sedimentary sequences, plant fossil data, and high-resolution spore-pollen data are indispensable.

Previous palaeontological and palaeobotanical research on the late Permian–Early Triassic transition in southwestern China indicates that the destruction of the peat-forming ecosystem dominated by the *Gigantopteris* flora occurred at the base of the Kayitou Formation [20, 87, 102]. During the deposition of the Kayitou Formation, the diversity of plant macrofossils decreased rapidly. Furthermore, many Mesozoic plants first appeared, and the plant assemblage transitioned to the *Annalepis-Peltaspermum* assemblage [87]. From the perspective of plant macrofossils, the vegetation turnover occurred in the lower part of the Kayitou Formation. However, this macrofossil data is too coarse to fully understand the response of terrestrial plants to the PTME. Additionally, plant macrofossils can be significantly influenced by lithology, thereby affecting the interpretation of terrestrial ecosystem disturbance [93, 103]. Some studies even suggest that no clear plant extinction occurred [104].

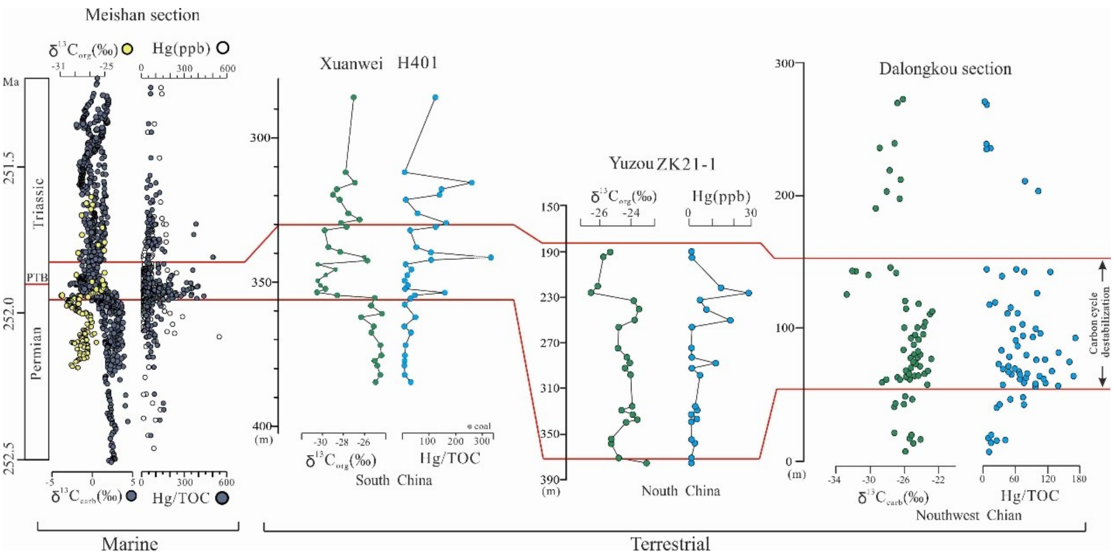

Figure 2. Relationship between marine and terrestrial strata established based on the anomaly of negative deviation of δ^{13}C and Hg concentrations. The destabilization range of the terrestrial carbon cycle is significantly larger than that of the marine carbon cycle. Data compilation from other references: Marine strata (Meishan section) [21], Xuanwei core H401 [19], Yuzhou core ZK21-1 [105] and Dalongkou section [43].

Previous palynological studies in southwestern China showed a sudden decrease in spore-pollen diversity above the last coal seam of the Xuanwei Formation [25, 95]. This interval of sharp decline in spore-pollen genera and species is considered the onset of forest collapse. However, the timing of terrestrial plant extinction is not as singular as described by macrofossils [99]. Moderately abundant plant fossils are still found in the lower Kayitou Formation at the Guanbachong section and in borehole cores from the Xuanwei coalfield [35, 81]. After the disappearance of the *Gigantopteris*-dominated rainforest ecosystem in the Mide and Lengqinggou sections of southwestern China, low-diversity plant populations immediately appeared [22, 93]. In the latest palynological research on southwestern China, the late Permian–Early Triassic is redivided into four spore-pollen assemblages [25], from bottom to top, *Tripartites cristatus var. minor*-*Torispora laevigata* (ML) *Crassispora orientalis*-*Anticapipollis tornatilis* (OT) *Lundbladispora communis*-*Aratrisporites yunnanensis* (CY) *Pteruchipollenites reticorpus*-*Protopinus fuyuanensis* (RF). The CY assemblage in the lower Kayitou Formation also shows the plants' response to the terrestrial ecosystem disturbance event. Notably, this study further investigated the overlying strata and found that pollen abundance and diversity both recovered after the terrestrial ecological crisis [25]. In the RF assemblage of the upper Kayitou Formation, gymnosperm pollen dominates, with the palaeobotanical community rich in *Alisporites*, *Protopinus*, and *Pityosporites*. Research indicates that this gymnosperm pollen primarily originated from upland areas rather than lowland swamp vegetation [93, 103]. Increasing aridity in the Early Triassic is generally considered a major threat to plant survival [3]. Therefore, drought-tolerant plants growing in uplands were likely the first to recover after the PTME, as they were pre-adapted to arid environmental conditions [93]. In southwestern China, herbaceous lycopsids inhabited coastal areas [22], while more drought-tolerant gymnosperms like conifers lived in uplands and survived the ecosystem disturbance across the Permian–Triassic transition.

Subsequently, in the upper Kayitou Formation and the Dongchuan Formation, the lithology gradually transitions to red clastic rocks, indicating an extremely arid palaeoclimate at that time [80]. This reddish lithology is widely distributed in non-marine strata of southwestern China and contains almost no spore-pollen fossils. This is likely due to the oxidation and disappearance of organic matter, including palaeobotanical remains after deposition, rather than the complete absence of plants during this period [92]. Alternatively, this phenomenon could be interpreted as the complete collapse of lowland terrestrial plant communities during this interval. In summary, although the main pulse of extinction did not completely destroy the terrestrial plant system, macro- and micro-fossil evidence of terrestrial vegetation in southwestern China completely disappears as Triassic aridity intensified. These findings contrast sharply with the short-term, sudden extinction process of marine biota and support the hypothesis that terrestrial plant extinction in southwestern China was a long-term, staged process [25].

However, the response of terrestrial vegetation to the extinction event clearly varied across different regions (Figure 3). Recent studies indicate that the terrestrial plant extinction process seems not to have been as brief and synchronous as that of marine organisms; the response of the terrestrial ecosystem crisis exhibited significant differences across latitudinal zones [13, 20]. In north China, the palaeoclimate gradually became arid as early as the Wuchiapingian Age, and peat swamps nearly disappeared regionally [51, 106]. The plant communities shifted to more drought-tolerant Euramerican flora [51, 107]. The terrestrial ecosystem crisis in north China occurred about 270 $\pm$ 150 kyr before the marine mass extinction [108], with an even earlier vegetation shift [105]. In southern Tibet, the PTME only caused short-term disturbance and range contraction in terrestrial plant communities, with terrestrial vegetation recovering within thousands of years [24]. In the Sydney Basin, the collapse of the *Glossopteris* flora might have occurred before 252.3 Ma [13]. Overall, the destructive impact of the PTME on terrestrial vegetation is reliably supported. However, this response was closely related to regional palaeoclimate and the types of existing plant taxa [109]. Due to its special geographical location, southwestern China maintained a relatively warm and humid climate during the late Permian, providing a last refuge for Paleozoic pteridophytes. Consequently, when global temperatures rose at the end of the Permian, the humid climate persisted, enhancing the ability to resist ecological and environmental pressures. This also contributed to the prolonged process of ecosystem disturbance in southwestern China. Given the divergent evolutionary trajectories of plants driven by distinct geographical settings, it is essential to consider palaeogeographic variations when discussing plant turnover.

3.3. Chronostratigraphic Framework of Terrestrial Strata

High-precision isotopic ages provide a tool for cross-facies and cross-regional correlation of the biotic crisis across the Permian–Triassic (P–T) boundary [4, 90]. As one of the most intensively studied regions for terrestrial PTME strata, south China has established a relatively precise temporal framework [14]. However, dating of volcanic ash layers only provides chronological points for comparing the sequence of extinction events; it cannot constrain the duration of the extinction, leaving the biotic crisis without precise temporal constraints.

In recent years, Milankovitch cyclostratigraphy has been widely used to analyze sedimentation rates in deep-time strata or to calibrate the timing of geological events. Establishing a reliable chronostratigraphic scale through this method offers the potential to constrain the duration of mass extinction events [19, 110]. Therefore, integrating cyclostratigraphic studies with biostratigraphic, chemostratigraphic, and U–Pb geochronological work helps determine the duration of ecosystem crises. This is significant for comprehensive understanding of ecosystem crises in geological history and predicting modern environmental changes.

Zircon U–Pb isotopic ages from volcanic ash layers and the negative carbon isotope excursion have become the most reliable means for identifying the end-Permian mass extinction event and determining the position of the PTB [21]. High-resolution natural gamma-ray (GR) logging data have been extensively used to analyze Milankovitch cycle periods recorded in strata. Building on this, combined with reliable absolute age dates, can further establish a relatively robust chronostratigraphic scale.

Previous research, using geochemical data and zircon ages from volcanic ash layers, once suggested the PTB was near the base of the Dongchuan Formation in southwestern China [80]. Conversely, chemostratigraphic and biostratigraphic data indicate the PTME horizon might be at the base or within the middle part of the Kayitou Formation [17, 25]. Recently reported high-precision ages from eight volcanic ash layers in the late Permian–Early Triassic transitional strata of southwestern China suggest the PTB is likely located at the top of the Xuanwei Formation or the base of the Kayitou Formation [14]. Plant macrofossil and palynological data indicate the collapse of the *Gigantopteris* flora swamp ecosystem occurred at the base of the Kayitou Formation [25, 92]. Zircon U–Pb ages (250.3 ± 2.1 Ma and 252.0 ± 2.1 Ma) from volcanic ash in the uppermost coal seam (C1) of the Xuanwei Formation, combined with carbon isotope shifts, suggest the PTB is located at the top of the Xuanwei Formation [63]. High-precision CA-ID-TIMS dating of volcanic ash from the C1 coal seam (251.93 ± 0.096 Ma and 252.29 ± 0.03 Ma) also supports this view (Figure 4).

Fluctuations in the stable carbon isotopes of organic matter reflect changes in the composition of atmospheric carbon dioxide and are often associated with ecosystem disturbances [85]. Since volcanic activity during the PTME period led to abrupt global ecological and environmental changes, the synchronicity of Hg concentration anomalies and carbon isotope fluctuations in strata can serve as one of the markers for stratigraphic correlation [17]. The combination of negative $\delta^{13}C_{org}$ excursions and Hg concentration anomalies provides a relevant chemostratigraphic tool for the extinction event. In recent research, the first negative $\delta^{13}C_{org}$ excursion and Hg/TOC peak appeared simultaneously in the Xuanwei H401 borehole core from southwestern China. Based on this, and combined with dating of volcanic ash from the C1 coal at the top of the Xuanwei Formation, the provisional astronomical timescale was assigned to a determined age, thereby establishing a stable timescale for the H401 core (Figure 4). Linking this time-calibrated core profile with the GSSP Meishan section, Figure 4 shows that the total duration of the carbon cycle perturbation (from the start of CIE-1 to the end of CIE-2) is approximately 660 kyr (1.5 long eccentricity cycles or 6.5 short eccentricity cycles) [19]. This result is slightly longer than the duration of carbon isotope perturbation in the Meishan carbonate rocks (427 ± 79 kyr) [8], but consistent with the cyclostratigraphic estimate of 600–700 kyr for the PTME duration in the Sichuan Shangsi section [53].

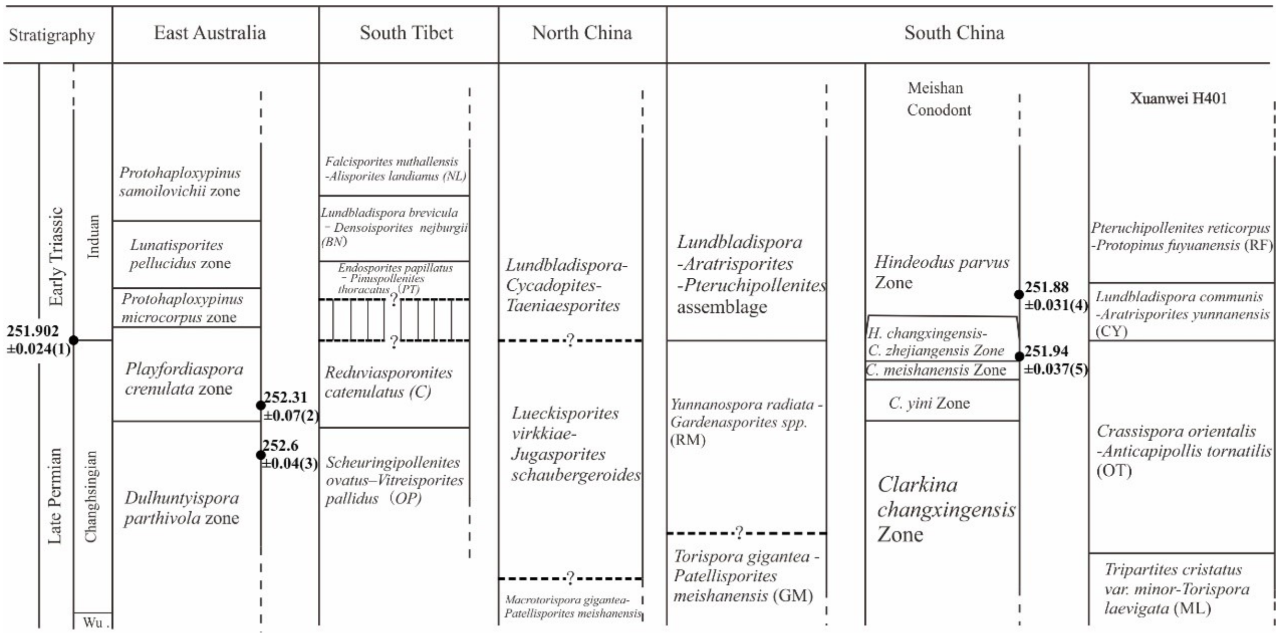

Figure 3. Correlation of the late Permian–Early Triassic palynostratigraphic scheme from epresentative sections of different regions. U/Pb ages (1), (4) and (5) from [89], U/Pb ages (2) and (3) from [14]. Data sources for palynostratigraphic schemes: Australia [13], southern Tibet [24], North China [105], and South China ([20, 25, 54] from left to right).

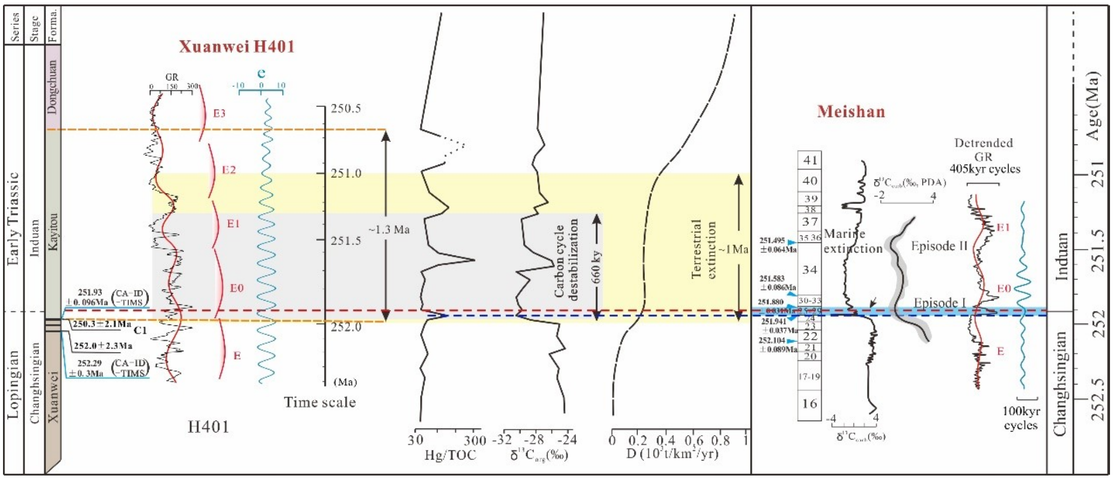

Figure 4. Astronomical cycle correlations between the marine Permian–Triassic global stratotype section at Meishan and the terrestrial records from Xuanwei core H401. Age data for Meishan are from Ref. [88]. $\delta^{13}C_{carb}$ data for Meishan are from Ref. [88] (**left panel**) and Ref. [57] (**middle panel**) and the astronomical cycles are from Ref. [110] (**right panel**). Age data for the Xuanwei core H401 are from Ref. [14]. Xuanwei core H401 data are from Ref. [19].

The main marine extinction phase in south China spans the *Clarkina meishanensis* and *Isarcicella isarcica* conodont zones in the Zhejiang Meishan section. Although statistical analysis of fossil data supports a single, brief catastrophic event [10], some studies have identified two extinction pulses near the PTB in marine strata of south China [55, 111]. Furthermore, increasing evidence suggests that terrestrial ecosystem disturbance in southwestern China might also have occurred in two phases [23, 55, 112, 113]. Recent data indicates that during the deposition of the Kayitou Formation, after a brief period of intense chemical weathering, the chemical weathering intensity decreased rapidly at the top of the Kayitou Formation and remained low throughout the Dongchuan Formation [19]. This weakening of chemical weathering of basalts in the Early Triassic might be related to accelerated physical erosion [15], a consequence of sparce vegetational cover and ground exposure following large-scale deforestation [39, 114]. Palynological data from southwestern China corresponds with the changes in erosion rates, further indicating a correlation between terrestrial ecosystem disturbance, vegetation destruction, and increased erosion rates. The erosion rate increased at the top of the Xuanwei Formation and increased again in the upper part of the Kayitou Formation. According to our astronomical timescale, these two increases are separated by an interval of approximately 1 Myr (Figure 4) [19]. Although the result of this astronomical cyclostratigraphic analysis is much longer than the marine extinction interval, it aligns with the duration of the terrestrial ecosystem crisis indicated by the *Lystrosaurus* fossil record in South Africa and elsewhere [79].

The lush tropical rainforests of the late Permian were the primary source material for coal formation in southwestern China and also provided habitats for contemporary animals [25]. The destruction of these forests would have severely disrupted non-marine ecosystems. Previous studies of plant macrofossils suggest that at the base of the Kayitou Formation, the flourishing pteridophyte flora was replaced by rapidly growing lycopsid communities [115]. The first phase of terrestrial ecosystem disturbance occurred at the base of the Kayitou Formation, characterized by the collapse of the pteridophyte-dominated flora and a rapid decline in plant diversity. However, as autotrophic primary producers, plants are not prone to sudden extinction, and a moderately diverse gymnosperm-dominated flora was quickly established [91]. Recent palynological data show a similar pattern, after a rapid decline in pteridophyte spores, a brief increase in gymnosperm pollen genera occurs in the middle part of the Kayitou Formation [25]. Despite its devastating nature, the first extinction pulse did not lead to the complete collapse of the terrestrial ecosystem in southwestern China. Growing evidence indicates that the large-scale deforestation event occurred not at the end of the Permian, but during the Induan Age of the Early Triassic [24, 116]. As aridity intensified in the Early Triassic, plants, unable to adapt to the prevailing environment, underwent a comprehensive collapse, corresponding to the second rise in terrestrial erosion rates observed in the Xuanwei H401 core in southwestern China. Although some studies indicate that a small number of gymnosperms persisted in upland areas [92], lowland regions had become barren landscapes by the early Triassic [22]. A second, more pronounced increase in erosion rates, accompanied by high physical erosion rates in the upper Kayitou Formation (Early Triassic), marks the complete collapse of the terrestrial plant ecosystem and the peak of terrestrial ecosystem disturbance in southwestern China [19]. Based on cyclostratigraphic analysis, the entire duration of the terrestrial PTME is estimated to be about 1 Myr, contrasting sharply with the marine biotic extinction, which potentially concluded within tens of thousands of years [10]. This prolonged terrestrial disturbance also likely influenced the marine extinction process; the terrestrial crisis led to increased surface runoff, potentially causing eutrophication and hypoxia in shallow marine areas, thereby propelling the marine environmental crisis. The final terrestrial ecosystem collapse occurred only after the marine extinction event had concluded, suggesting the relationship between terrestrial and marine losses is more complex than previously thought. The terrestrial ecosystem, being in direct contact with volcanism-induced climate changes, might have responded relatively early. However, vegetation, as primary producers, has a relatively high capacity to cope with environmental changes and can adapt to relatively harsh climatic conditions. The presence of vegetation means habitat and food sources for terrestrial organisms, preventing their immediate complete extinction. Therefore, the terrestrial biotic extinction process was likely more protracted than that in the marine realm [20].

4. Palaeowildfires and their Impact on Terrestrial Ecosystems Collapse at the P–T Transition

4.1. Wildfire Records and Ecological Roles

Wildfires have been widely studied and reported in both modern and geological history. Modern data indicate that over 80% of the global land surface has experienced burning [26, 44, 45]. Frequent forest fires are considered a potential significant factor in climatic shifts and biotic extinctions within Earth's cycles [28, 29]. Since plants colonized land in the Silurian, evidence of wildfires has been found associated with major climatic turning points in geological history [41, 97, 117]. Wildfires themselves possess immense destructive power, capable of devastating vegetation in short periods. Post-fire events can also lead to regional environmental degradation, threatening the survival of animals and plants [28, 118]. The PTME is the most severe mass extinction event of the Phanerozoic, and evidence of wildfires has been widely reported from strata associated with this event [37, 40, 119]. Statistical analyses reveal that an increase in wildfire frequency during the Permian–Triassic transition was a global phenomenon [37, 120]. Previous research suggested that these globally frequent wildfires may have directly or indirectly caused terrestrial ecosystem disturbance during the PTME [81]. Evidence for palaeowildfires in the Permian–Triassic transition is found not only in terrestrial strata but also in marine strata with charcoal and polycyclic aromatic hydrocarbons [5, 41, 121].

The three essential elements for wildfire are oxygen, fuel (vegetation), and ignition sources. Additionally, various natural conditions, including climate, influence wildfire scale, and type. Previous studies suggest late Permian atmospheric oxygen levels were as high as 27% [29, 30]. Concurrently, abundant terrestrial vegetation provided the material basis for the occurrence and spread of wildfires, while increasingly arid climates further promoted their prevalence [122]. Therefore, by the end of the late Permian, wildfires could occur rapidly on a global scale, damaging terrestrial ecosystems in short order. They also released large quantities of harmful substances like carbon dioxide, aerosols, and polycyclic aromatic hydrocarbons, potentially causing global terrestrial ecosystem disturbance [31, 123]. However, some scholars remain skeptical about the scale and massive impact of wildfires, arguing that they are a relatively common phenomenon in natural ecosystems and unlikely to directly cause global terrestrial ecosystem collapse. Inferring from the scale of modern forest fires, clearly, a single wildfire event could not lead to ecosystem disturbance in a short time [26]. Currently, multiple mechanisms are proposed for terrestrial ecosystem disturbance during the PTME, including acid rain, ozone layer depletion, and global warming, all attributed to large emissions of toxic and harmful substances from volcanic activity [21]. Wildfires might be viewed as a consequence triggered by abrupt environmental changes rather than a causation mechanism initiating ecosystem disturbance. The premise for wildfire events causing terrestrial ecosystem disturbance during the Permian–Triassic transition relies on three conditions. Firstly, late Permian atmospheric oxygen levels reached exceptional highs, a crucial condition enabling sustained burning and spread of wildfires [124]. Secondly, the arid climate made forests more combustible with build-ups of readily available fuel. Finally, frequent regional or global volcanic activity accelerated environmental deterioration, making wildfires one of the primary destructive forces for terrestrial ecosystems at that time [27, 28].

It remains problematic to convincingly attribute terrestrial ecosystem disturbance primarily to wildfires, a natural phenomenon. However, linking large-scale, frequent wildfires to the fragile ecological environment weakened by concurrent volcanic activity seems to explain their destructive potential in that context [125]. In Permian–Triassic transitional strata, anomalies in volcanic indicators like Hg concentrations have been extensively reported, indicating intense volcanic activity. In the Xuanwei H401 borehole core from southwestern China, the anomalous Hg/TOC interval corresponds with peaks in inertinite, demonstrating a connection between the two [40]. Frequent volcanism, including regional events and the Siberian Traps Large Igneous Province, began as early as the late Permian [7]. Initially, environmental changes did not exceed the self-regulating capacity of ecosystems, and terrestrial and marine ecosystems did not respond drastically, though ecological stress undoubtedly increased. Palaeowildfire events could have acted as a crucial catalyst for terrestrial ecosystem disturbance during the Permian–Triassic transition, accelerating the process of environmental deterioration. Therefore, wildfires during this transition played a significant role in terrestrial ecosystem disturbance, and in the transformation of the entire ecosystem. Recent research suggests that plant evolution and the biotic extinction during the PTME were not singular events but likely occurred in multiple phases, and the evolution of wildfire types also shows multiple stages [40, 123]. To further dissect the role of wildfires in different stages, more detailed research is needed to link wildfire types with specific phases of plant and ecosystem disturbance.

4.2. The Link between Palaeowildfires and Plant Evolution

4.2.1. Wildfire Occurrence Conditions During the Permian–Triassic Transition

Frequent wildfire events can destabilize forest systems in a short period, which is catastrophic for the vegetation itself [28]. Conversely, plants, as the combustible material base, are a prerequisite for the occurrence of wildfire events. The late Permian–Early Triassic transition was also a turning point for terrestrial vegetation types. The frequent wildfires at the end of the Permian, while destructive, may have, to some extent, also driven plant evolution. Conversely, changes in plant communities might have led to variations in wildfire types [45]. Therefore, while discussing the destructive impact of wildfires on plants, we should also consider the link between wildfires and vegetation turnover.

During the late Permian, the southwestern region of China was one of the world's important coal-producing areas, providing ample fuel such as plants and peat [35]. Furthermore, atmospheric oxygen concentrations have been reported to be as high as 27%, significantly above the modern level of 21% [124, 126]. However, the tropical rainforests near the equator, characterized by year-round rainfall, are typically dense and humid environments, seemingly not so prone to burning. Under modern, normal natural conditions, large-scale forest fires do not occur in tropical rainforests; the frequent wildfires in the Amazon rainforest in recent years are largely anthropogenic [127]. Therefore, an ignition source is crucial for tropical rainforests to burn. The high-temperature pyroclastic materials released by volcanic eruptions were highly likely a significant ignition source for the late Permian tropical rainforests in south China. However, if volcanic activity served as the forest ignition source, the volcanoes could not be as distant as the Siberian Traps Large Igneous Province. Recently, regional volcanic island arcs in south China during the late Permian–Early Triassic transition have become a hot topic of discussion [128]. This research suggests that regionally erupted felsic volcanism might have triggered the mass extinction across the P–T boundary in south China, which is also evidenced by the widely distributed volcanic ash layers in south China [9, 62]. Therefore, felsic volcanism in southwestern China was likely a significant ignition source for the frequent wildfires in the *Gigantopteris* tropical rainforests. Additionally, volcanic eruptions also release large amounts of greenhouse and harmful gases. The rapid temperature increase caused by greenhouse gases can lead to arid climates, which also increases the frequency of forest fires [44, 129]. In modern forest landscapes, seasonal drought and high temperatures lead to increased frequencies of forest wildfires [130]. Furthermore, studies have indicated that CO_2 released by volcanic eruptions can increase lightning frequency [27]. Lightning has been a major cause of forest wildfires throughout geological history. Consequently, palaeovolcanic eruptions in south China could have driven large-scale wildfire events through multiple pathways.

4.2.2. Coupling of Wildfire Types and Vegetation Succession

Wildfire types are closely related to vegetation conditions [28]. Generally, dense, and complex multi-layered vegetation supports various types of wildfires during combustion, whereas relatively barren vegetation conditions result in more specific wildfire types. Due to the palaeogeographic location of the study area, southwestern China had a humid climate in the latest Permian, serving as the last refuge for the Paleozoic pteridophyte-dominated Cathaysian Flora (the *Gigantopteris* group) [25, 92]. The South China Block was widely covered by late Permian peat-forming plant ecosystems, dominated by *Gigantopteris* and *Gigantonoclea*. These plants thrived, along with *Lobatanularia*, *Paracalamites*, and *Pecoperis*, in a warm and humid tropical climate, providing abundant fuel for wildfire events. However, in modern closed broadleaf forests, litter decomposes easily under persistently dark and humid conditions, and the initial environment is often moist, reducing plant flammability [67]. This situation suppresses wildfires and leads these closed forests to be typically considered fire-resistant [127, 131], although they still include some flammable species [132].

Although the relatively high atmospheric oxygen concentration in the late Permian facilitated wildfire ignition and spread, the initial wildfires were likely low-intensity, occurring as ground or subsurface fires [28, 39]. These types of fires spread relatively slowly, typically smoldering around tree bases and occurring in a highly embedded manner [119]. Furthermore, anomalous warming and short-term reductions in precipitation during the late Permian may have promoted and sustained wetland fires [65]. In this context, once rainforests were burned, the community structure changed, affecting the relative environmental humidity and making vegetation more susceptible to intense wildfires [28]. These studies provide important context for interpreting the inferred changes in wildfire types observed in the Xuanwei H401 bore core sequence from southwestern China, particularly in the upper part of the Xuanwei Formation (Stages 1 and 2 in Figure 5).

In the early late Permian, due to the humid climatic environment of the rainforests, wildfires were less frequent, primarily distributed in decaying litter, spread slowly, and were dominated by surface or subsurface fires. As volcanic activity intensified globally or regionally, decreased rainfall and seasonal arid climates led to accelerated wildfire spread within forests. By the end of the Permian, wildfires had gradually evolved to include high-temperature crown fires with high combustion temperatures and strong destructive power. Crown fires, with their ultra-fast spread rates, rapidly spread through entire forests, damaging the terrestrial forest ecosystem in a short time. The increase in frequent and intense wildfires in the latest Permian likely affected the last wetland communities, represented by the uppermost coal seam in the Xuanwei Formation (Stage 2 in Figure 5), leading to the extinction of many plant and animal species.

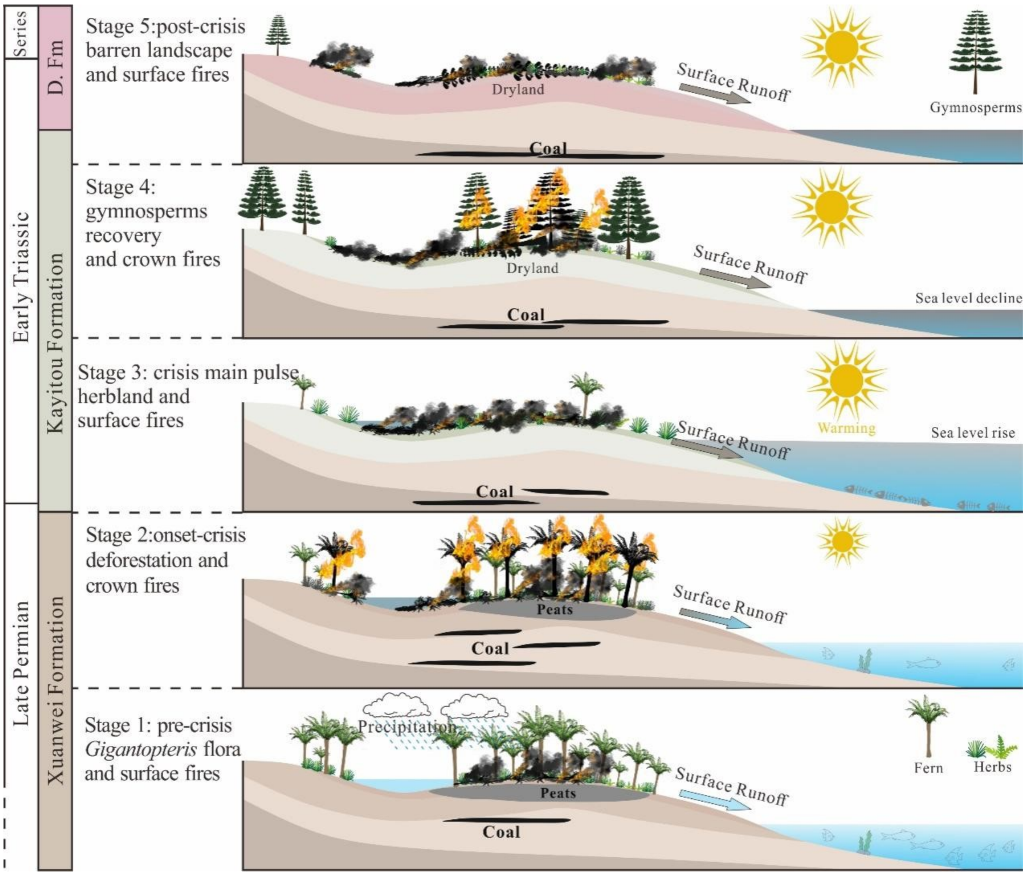

Figure 5. Schematic model illustrating possible relationships between the wildfires and floral changes during the Permian–Triassic transition in southwestern China. Modified after Ref. [40].

Peaks in inertinite content occur at the base of the Kayitou Formation and are associated with relatively low inertinite reflectance, negative $\delta^{13}C_{org}$ excursions, and sedimentary Hg peaks. Palaeontological investigations indicate that vegetation changes in southwestern China occurred above the last coal seam of the Xuanwei Formation [25, 39]. In the lower Kayitou Formation, remnants of the *Gigantopteris* flora, together with Triassic plant fossils like *Tomiostrobus* (*Annalepis*), form a distinctive *Annalepis-Peltaspermum* assemblage [87]. During the deposition of the lower Kayitou Formation, the palaeogeographic environment had become a near-barren landscape dominated by herbaceous plants [22]. Under these conditions, although anomalously high temperatures from concurrent Siberian Traps Large Igneous Province (STLIP) volcanic activity increased wildfire frequency, the wildfire type was limited to surface fires due to the lack of combustible material, with no high-temperature crown fires occurring (Stage 3 in Figure 5).

Recent botanical studies show that after the terrestrial plant crisis event, plants experienced moderate recovery with increases in the abundance and diversity of gymnosperms and ferns [25, 115]. A flora dominated by drought-tolerant conifers gradually replaced the pteridophyte-dominated communities. The latest spore/pollen ratio analysis in palynological studies indicates that the relative abundance of pollen increased and gradually became dominant in the upper Kayitou Formation [25]. It is important to note that pollen dominance is common after frequent surface fires, possibly because wildfires cleared opportunistic plant species following the PTME, freeing up ecological niches for gymnosperm recovery. In the early Early Triassic, as gymnosperms gradually occupied the available niches during the deposition of the lower Kayitou Formation, the opportunistic lycopsid *Tomiostrobus* was eventually replaced after the sharp reduction in plant genera and species [87, 115]. Likely due to the increase in gymnosperms, wildfire fuel became abundant again. By the time of deposition of the middle Kayitou Formation, high-temperature crown fires had resumed (Stages 4 in Figure 5). Although there is no irrefutable evidence that these gymnosperms were tall woody plants [92], the higher inertinite reflectance values and the inferred higher combustion temperatures are consistent with crown fires. This, in turn, suggests that the plants at that time were not limited to low herbaceous types [41]. As global warming and increasing aridity further threatened the Early Triassic terrestrial ecosystems, the development of drought-tolerant, gymnosperm-dominated communities was also constrained, and biodiversity plummeted. Finally, widespread plant extinction occurred during the deposition of the upper Kayitou Formation (Figure 5).

In summary, research shows that wildfires are not only destructive but also intrinsically linked to vegetation renewal and change, impacting terrestrial ecosystems. After terrestrial ecosystem disturbance reached its peak, by the time of the Dongchuan Formation deposition, the palaeogeographic environment in southwestern China had evolved into a nearly barren landscape [92]. By this stage, crown fires had subsided, and subsurface and surface fires likely impacted on the last remaining flora during the deposition of the upper Kayitou Formation (Stage 5 in Figure 5).

The relationship between wildfires and plants is not purely destructive. While wildfire types are controlled by climatic conditions, they are also influenced by plant types. As primary producers, although affected by geographical location and climate, plants demonstrated remarkable resilience under frequent wildfire events and the harsh environmental conditions of the time. Wildfires could clear out Paleozoic pteridophytes, providing numerous ecological niches for plant evolution and promoting plant development. This is also one of the important roles' wildfires play in the natural world today [26, 132]. Thus, during the Permian–Triassic transition, palaeowildfire events exhibited not only destructive power but also contributed to plant evolution.

4.3. The Influential Role of Palaeowildfires in P–T Terrestrial Ecosystem Disturbance

4.3.1. Spatiotemporal Distribution and Evidence of Wildfires

Some drivers of terrestrial ecosystem disturbance, such as acid rain and ozone layer destruction, are inferred from indirect and often localized evidence [21]. In contrast, evidence for wildfire events indicates they occurred globally during the PTME, with traces found not only in terrestrial strata of the PTME interval but also in marine sections like the GSSP at Meishan [4, 121]. Consequently, intensified wildfires are often considered a key component of the terrestrial PTME.

Wildfires not only directly destroy forest systems but also release harmful gases and particulate matter into the atmosphere, posing potentially devastating impacts on terrestrial ecosystems [44, 65]. The destruction of surface vegetation by wildfires can lead to increased soil erosion (Figure 1), transporting large amounts of sediment into marine ecosystems through surface runoff [23, 39]. Published data show high abundances of inertinite and polycyclic aromatic hydrocarbons (PAHs) in the latest Permian coal seams [31, 80, 106, 119]. This suggests that wildfire activity persisted for a longer duration than the terrestrial ecosystem collapse itself, raising questions about the precise relationship between wildfires and the terrestrial PTME. Figure 6 integrates data from multiple sections in south China, including the Meishan GSSP section. We utilize this correlation to assess the link between wildfires and changes in the terrestrial ecosystems (Figure 6). The co-occurrence of the negative δ^{13}C excursion and Hg/TOC peaks during the PTME provides a useful tool for correlation between different terrestrial and marine records. Based on this correlation, wildfire events were widespread in south China over an extended period, both before and after the main pulse of the marine biotic crisis (Figure 6).

4.3.2. Phased Destruction of Ecosystems by Wildfires

Several previous studies have suggested that wildfires played a significant role in terrestrial ecosystem destruction during the PTME, potentially causing the collapse of the peat-forming ecosystems in southwestern China during the late Permian [39]. The analysis presented here indicates that during the Permian–Triassic transition, intense wildfires might not have suddenly and completely eradicated plants within a very short interval. Instead, wildfires likely played a significant role in driving forest transformation. Conversely, forest evolution probably controlled wildfire types. Today, forest fires are prevalent, and wildfire occurs regularly across much of the Earth's surface [26]. However, the prevailing view is that wildfires do not typically lead to the complete collapse of forest ecosystems [28].

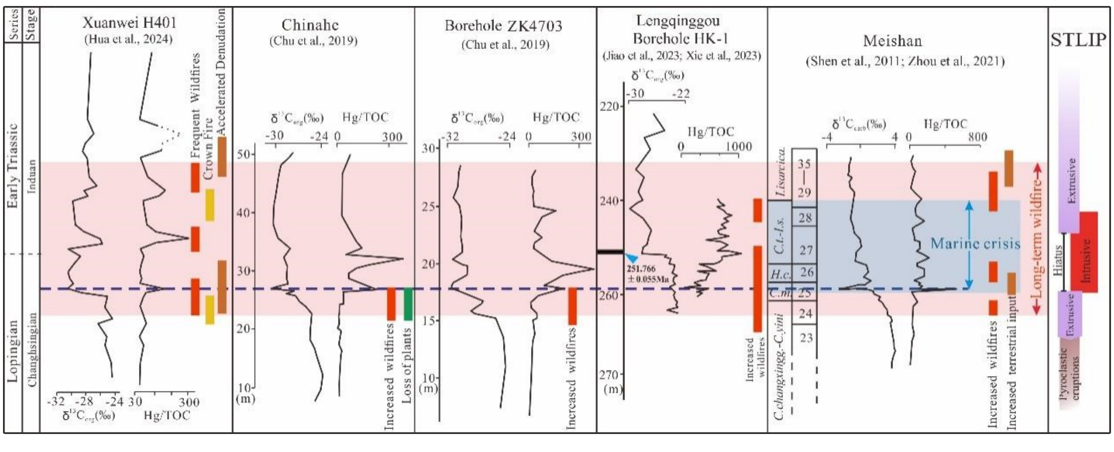

Figure 6. Compilation of $\delta^{13}C_{org}$, Hg/TOC ratios and wildfire activities through the Permian–Triassic transition in south China. The data from Chinahe and ZK4703 is from from Ref. [17]; the data of Lengqinggou is from Ref. [14]. $\delta^{13}C_{org}$ and Hg/TOC data from Meishan is from Ref. [61]; and wildfires and terrestrial input at Meishan is from Ref. [121]. The magmatic phases of the STLIP are from Ref. [7]. Xuanwei core H401data are from Ref. [40].

Recent studies on the timing of the PTME indicate significant differences in the response times and processes of terrestrial ecosystems across different latitudes [13, 14, 106, 108]. Although wildfires themselves seem unlikely to completely disrupt terrestrial ecosystems, the gradual intensification of wildfires in the late Permian may have made terrestrial forest systems more vulnerable to stresses from other factors. The first phase of terrestrial ecosystem disturbance coincides with the initial pyroclastic eruption phase of the STLIP [7]. Wildfires, along with the initial volcanic activity, potentially causally linked, clearly contributed to the earlier disturbance in terrestrial, compared to marine, environments.

In the latest Permian, wildfires destabilized forest systems. Furthermore, vegetation combustion released large amounts of pollutants like carbon dioxide and polycyclic aromatic hydrocarbons, affecting the carbon cycle and regional climate [55, 123]. Following wildfire events, the loss of vegetation cover exacerbated surface runoff and erosion [15, 19, 31]. It is hypothesized that large amounts of terrestrial clastics and wildfire residues were transported by rivers into the oceans, leading to increased water turbidity and marine productivity [39, 133]. However, the lack of organic-rich mudstones (black shales) in the Permian–Triassic transitional strata of southwestern China to substantiate this process led Wignall et al. to suggest that organic matter was distributed within alluvial and fluvial facies due to marine transgression influences [11]. Therefore, terrestrial ecosystem disturbance events likely caused ecological stress in the oceans even before the complete collapse of terrestrial ecosystems. The subsequent intrusive phase of the STLIP delivered a substantial blow to the already fragile ecosystem, with the ensuing 8–10 °C warming sufficient to kill most marine life [134]. During this phase, frequent surface fires cleared the last Paleozoic plant communities, creating niches for the development of new Mesozoic flora. In the Early Triassic, drought-tolerant gymnosperms gradually became the dominant group as temperatures and precipitation patterns changed. Throughout this transition, persistently frequent wildfires and volcanic activity likely delayed the full recovery of terrestrial ecosystems. Ultimately, the even harsher environments of the later Early Triassic eradicated the last gymnosperms in southwestern China, leading to a second acceleration in erosion rates [19, 23, 121]. If plants provided combustible material, wildfire activity appears to have persisted. While wildfires might not have directly caused the global PTME, an indirect link between them likely exists.

4.3.3. Comprehensive Impact Mechanism of Wildfires on Ecosystems

STLIP and contemporaneous volcanically driven environmental changes are often considered the primary causes for the biotic extinction across the P–T transition. Numerous studies indicate that volcanic activity can trigger catastrophic global environmental changes (e.g., global warming) by releasing CO_2, SO_2, other volatiles, and toxic metals, many of which have been identified in PTME research [9, 61, 67]. Global warming, anoxia, and ocean acidification are directly linked to the marine biotic crisis [21]. The main intrusive phase of the STLIP and its associated massive greenhouse gas emissions occurred at 251.907 $\pm$ 0.067 Ma, correlating with the mass extinction event recorded in marine strata within an interval of less than 100 kyr [10, 110]. As shown in Figure 6, the close correspondence between Hg/TOC peaks and stable carbon isotope fluctuations during the Permian–Triassic transition suggests volcanic activity released vast quantities of light isotope CO_2 ($\sim$36,000 Gt C) into the oceans and atmosphere during this period [135, 136]. Greenhouse gases released by volcanic activity caused extreme global warming, with sea surface temperatures reaching 40 °C [135, 136], leading to the catastrophic mass extinction event.

The marked increase in erosion rates indicates intense changes in the terrestrial hydrological cycle (Figure 7), which, combined with the seasonally extreme high temperatures, may have further promoted aridity on land [65]. Consequently, frequent and intense wildfires could have been a significant factor in global warming [129]. Beyond the palynological data from southwestern China, abundant wildfire-generated charcoal is also found in Permian–Triassic strata elsewhere on the South China Block, such as seen on the North China Block [106, 137], and in eastern Australia [31, 119]. Given regional differences in climate and biota, this prevalence of wildfires was likely induced by volcanically driven global climate change, including warming and enhanced seasonality.

In multiple studies, horizons rich in inertinite or PAHs coincide with Hg/TOC peaks, suggesting a causal link between volcanic activity and wildfires [40]. In the modern era, nearly 1.4 billion lightning strikes occur globally each year, with frequency increasing as the climate warms [27]. Global warming during the P–T transition may have significantly increased lightning frequency, leading to more frequent forest fires. Zhang et al. proposed that large-scale felsic volcanic eruptions during the P–T transition injected large amounts of S, Cu, and Hg into the south China region, potentially causing regional ecosystem disturbance [9]. Volcanic pyroclastics released by regional eruptions could also have been a significant ignition source in forests. The widely distributed volcanic ash layers in the late Permian-Early Triassic strata of south China also support the scenario where regional volcanic activity exacerbated regional wildfire activity. Therefore, volcanic activity both around the South China Block and from the STLIP appears to have driven climate shifts and wildfire events, causing irreversible damage to terrestrial ecosystems during the Permian–Triassic transition.

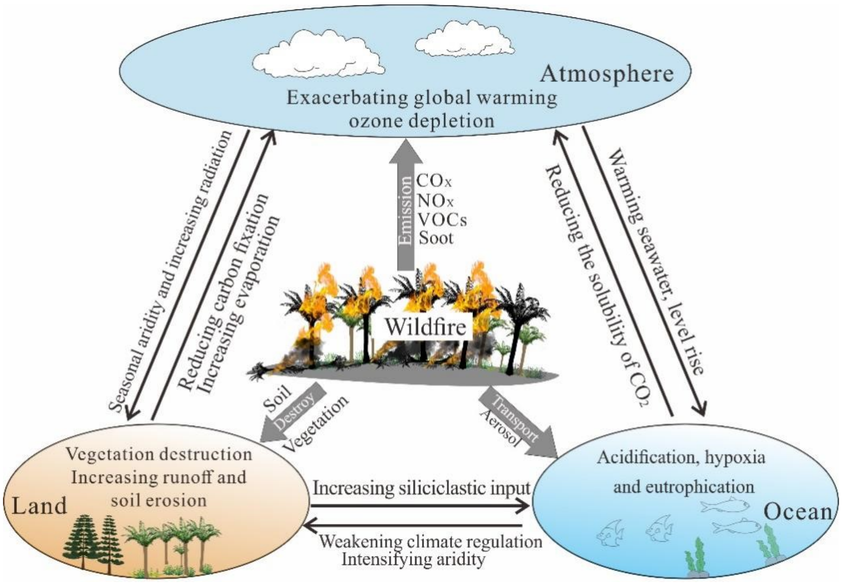

Figure 7. The relationships between wildfires and the atmosphere, land, and oceans.

In summary, the impact of wildfires on ecosystems manifests in multiple ways (Figure 7). Enhanced wildfire activity destroyed animal habitats while generating large amounts of CO_2, soot, PAHs, etc., leading to ecological deterioration [65]. After forest combustion, exposed land due to vegetation loss, coupled with a disrupted hydrological cycle, led to severe soil erosion [31, 39]. Large quantities of terrestrial clastics entering the oceans through rivers caused seawater eutrophication, increasing pressure on marine ecosystems [31, 39]. Wildfires were a crucial component in the process of ecosystem disturbance and a significant factor leading to the gradual collapse of ecosystems [29].

5. Outlook

In summary, the PTME event, as a critical turning point in climate, ecology, and biological evolution during geological history, has become a subject of intense interest in current sedimentology research. While previous studies have yielded substantial insights, divergent viewpoints persist, necessitating further investigation,

1. Research on the marine PTME has largely converged on a unified view. A sudden and brief extinction process, extremely high extinction rates, and multiple superimposed extinction mechanisms have gradually formed the extinction model for marine life during the Permian–Triassic transition. However, constrained by regional palaeogeography, a unified model for terrestrial strata has not been established. The timing of the terrestrial ecosystem crisis interval remains controversial across different sections, and the process of terrestrial ecosystem disturbance urgently requires more in-depth research.

2. There are significant differences between the processes of the PTME event in terrestrial and marine strata, making their correlation a persistent challenge in academia. With the reporting of high-precision zircon U–Pb ages from volcanic ash layers, cross-facies stratigraphic correlation has become possible, and a high-resolution stratigraphic framework is gradually being refined. The integration of negative carbon isotope excursions, cyclostratigraphy, and zircon geochronology provides an approach for establishing a stable chronostratigraphic scale. The chronological framework for late Permian–Early Triassic terrestrial strata will benefit from further refinement.

3. As one of the last refuges for Paleozoic pteridophytes, southwestern China records the crucial process of plant transition during the PTME. Previous studies on plant fossils have established plant assemblages before and after the terrestrial ecosystem crisis and preliminarily reconstructed the vegetation landscape. However, with deeper research, the terrestrial ecosystem disturbance during the Permian–Triassic transition appears to have been a prolonged and multi-stage process. Therefore, previous studies might not fully cover the entire terrestrial disturbance processes, and the stages of terrestrial vegetation evolution across the P–T transition still require further investigation.

4. Frequent palaeowildfire events during the Permian–Triassic transition played a significant role in the terrestrial ecosystem disturbance processes. However, most research on palaeowildfire events remains at the level of discovery. Wildfires likely played different roles at various stages and held an important connection with vegetation evolution, but these conclusions are largely qualitative. Research on palaeowildfire events lack quantitative analytical results.

Recent quantitative studies on CO_2 emissions from volcanic activity during the Permian–Triassic ecosystem disturbance offer an approach for palaeowildfire research. Therefore, future studies could include the utilization of mathematical models to quantitatively assess the contribution of palaeowildfire events to the terrestrial ecosystem disturbance process.

Acknowledgements

This study was supported by the Key Project of the National Natural Science Foundation of China (No. 42530208) and the National Science and Technology Oil & Gas Major Project (2025ZD1405700).

Author Contributions

L.S.: Writing—review & editing, Writing—original draft, Supervision, Project administration, Funding acquisition, Formal analysis, Conceptualization. F.H.: Writing—review & editing, Writing—original draft, Methodology, Investigation, Formal analysis, Visualization. T.P.J.: Writing—review & editing, Conceptualization. T.Z.: Writing—review & editing, Methodology, Investigation. X.W.: Writing—Methodology, Investigation, Formal analysis. Z.Y.: Methodology, Investigation, Visualization. J.L.: Writing—review & editing, Methodology, Conceptualization. J.H.: Writing—review & editing, Conceptualization.

Funding

This research received no external funding.

Institutional Review Board Statement

Not applicable.

Informed Consent Statement

Not applicable.

Data Availability Statement

No new data were created or analyzed in this study. All data supporting the findings of this review are derived from previously published studies, which are cited in the reference list.

Conflicts of Interest

The authors declare that they have no known competing financial interests or personal relationships that could have appeared to influence the work reported in this paper.

Use of AI and AI-assisted Technologies

The authors declare that no artificial intelligence or AI-assisted technologies were used in the preparation of this manuscript.

References

1. Barnosky, A.D.; Matzke, N.; Tomiya, S.; et al. Has the Earth's sixth mass extinction already arrived? *Nature* **2011**, *471*, 51–57. https://doi.org/10.1038/nature09678
2. Plumptre, A.J.; Baisero, D.; Belote, R.T.; et al. Where might we find ecologically intact communities? *Front. For. Flob. Change* **2021**, *4*, 626635. https://doi.org/10.3389/ffgc.2021.626635
3. Algeo, T.J.; Shen, J. Theory and classification of mass extinction causation. *Natl. Sci. Rev.* **2024**, *11*, 237. https://doi.org/10.1093/nsr/nwad237
4. Benton, M.J.; Newell, A.J. Impacts of global warming on Permo-Triassic terrestrial ecosystems. *Gondwana Res.* **2014**, *25*, 1308–1337. https://doi.org/10.1016/j.gr.2012.12.010
5. Shen, S.Z.; Crowley, J.L.; Wang, Y.; et al. Calibrating the end-Permian mass extinction. *Science* **2011**, *334*, 1367–1372. https://doi.org/10.1126/science.1213454
6. Retallack, G.J. Permian and Triassic greenhouse crises. *Gondwana Res.* **2013**, *24*, 90–103. https://doi.org/10.1016/j.gr.2012.03.003
7. Burgess, S.D.; Muirhead, J.D.; Bowring S.A. Initial pulse of Siberian Traps sills as the trigger of the end-Permian mass extinction. *Nat. Commun.* **2017**, *8*, 164. https://doi.org/10.1038/s41467-017-00083-9
8. Wignall, P.B. Large igneous provinces and mass extinctions. *Earth-Sci. Rev.* **2001**, *53*, 1–33. https://doi.org/10.1016/S0012-8252(00)00037-4
9. Zhang, H.; Zhang, F.; Chen, J.B.; et al. Felsic volcanism as a factor driving the end-Permian mass extinction. *Sci. Adv.* **2021**, *7*, eabh1390. https://doi .org /10 .1126 /sciadv.abf8142.
10. Shen, S.Z.; Ramezani, J.; Chen, J.; et al. A sudden end-Permian mass extinction in south China. *Geol. Soc. Am.* **2019**, *131*, 205–223. https://doi.org/10.1130/B31909.1
11. Wignall, P.B.; Chu, D.L.; Hilton, J.M.; et al. Death in the shallows, the record of Permo-Triassic mass extinction in paralic settings, southwest China. *Glob. Planet. Change* **2020**, *189*, 103176. https://doi.org/10.1016/j.gloplacha.2020.103176
12. Davydov, V.I.; Karasev, E.V.; Nurgalieva, N.G.; et al. Climate and biotic evolution during the Permian-Triassic transition in the temperate Northern Hemisphere, Kuznetsk Basin, Siberia, Russia. *Palaeogeogr. Palaeoclimatol. Palaeoecol.* **2021**, *573*, 110432. https://doi.org/10.1016/j.palaeo.2021.110432
13. Fielding, C.R.; Frank, T.D.; McLoughlin, S.; et al. Age and pattern of the southern high-latitude continental end-Permian extinction constrained by multiproxy analysis. *Nat. Commun.* **2019**, *10*, 385. https://doi.org/10.1038/s41467-018-07934-z
14. Wu, Q.; Zhang, H.; Ramezani, J.; et al. The terrestrial end-Permian mass extinction in the paleotropics postdates the marine extinction. *Sci. Adv.* **2024**, *10*, 7284. https://doi.org/10.1126/sciadv.adi7284
15. Yang, J.H.; Cawood, P.A.; Condon, D.J.; et al. Anomalous weathering trends indicate accelerated erosion of tropical basaltic landscapes during the Permo-Triassic warming. *Earth Planet. Sci. Lett.* **2022**, *577*, 117256. https://doi.org/10.1016/j.epsl.2021.117256
16. Shen, S.Z.; Zhang, F.F.; Wang, W.Q.; et al. Deep-time major biological and climatic events versus global changes, Progresses and challenges. *Chin. Sci. Bull.* **2023**, *69*, 268–285. https://doi.org/10.1360/tb-2023-0218
17. Chu, D.L.; Grasby, S.E.; Song, H.J.; et al. Ecological disturbance in tropical peatlands prior to marine Permian-Triassic mass extinction. *Geology* **2020**, *48*, 288–292. https://doi.org/10.1130/G46631.1
18. Shen, J.; Yin, R.; Algeo, T.J.; et al. Mercury evidence for combustion of organic-rich sediments during the end-Triassic crisis. *Nat. Commun.* **2022**, *13*, 1307. https://doi.org/10.1038/s41467-022-28891-8

19. Hua, F.H.; Shao, L.Y.; Zhang, T.C.; et al. An astronomical timescale for the Permian-Triassic mass extinction reveals a two-step, million-year-long terrestrial crisis in South China. *Earth Planet. Sci. Lett.* **2023**, *605*, 118035. https://doi.org/10.1016/j.epsl.2023.118035

20. Ouyang, S. Upper Permian and Lower Triassic palynomorphs from eastern Yunnan, China. *Can. J. Earth Sci.* **1982**, *19*, 68–80. https://doi.org/10.1139/e82-006

21. Dal Corso, J.; Song, H.J.; Callegaro, S.; et al. Environmental crises at the Permian–Triassic mass extinction. *Nat. Rev. Earth Environ.* **2022**, *3*, 197–214. https://doi.org/10.1038/s43017-021-00259-4

22. Feng, Z.; Wei, H.B.; Guo, Y.; et al. From rainforest to herbland, New insights into land plant responses to the end-Permian mass extinction. *Earth-Sci. Rev.* **2020**, *204*, 103153. https://doi.org/10.1016/j.earscirev.2020.103153

23. Huang, Y.F.; He, W.H.; Liao, W.; et al. Two pulses of increasing terrestrial input to marine environment during the Permian–Triassic transition. *Palaeogeogr. Palaeoclimatol. Palaeoecol.* **2022**, *586*, 110753. https://doi.org/10.1016/j.palaeo.2021.110753

24. Liu, F.; Peng, H.P.; Bomfleur, B.; et al. Palynology and vegetation dynamics across the Permian–Triassic boundary in southern Tibet. *Earth-Sci. Rev.* **2020**, *209*, 103278. https://doi.org/10.1016/j.earscirev.2020.103278

25. Shao, L.Y.; Hua, F.H.; Wang, J.; et al. Palynological dynamics in the late Permian and the Permian–Triassic transition in southwestern China. *Palaeogeogr. Palaeoclimatol. Palaeoecol.* **2023**, *619*, 111540. https://doi.org/10.1016/j.palaeo.2023.111540

26. Bowman, D.M.; Balch, J.K.; Artaxo, P.; et al. Fire in the Earth system. *Science* **2009**, *324*, 481–484. https://doi.org/10.1007/978-90-481-8716-4_3

27. Chen, Y.; Romps, D.M.; Seeley, J.T.; et al. Future increases in Arctic lightning and fire risk for permafrost carbon. *Nat. Clim. Change* **2021**, *11*, 404–410. https://doi.org/10.1038/s41558-021-01011-y

28. He, T.H.; Lamont, B.B. Baptism by fire, the pivotal role of ancient conflagrations in evolution of the Earth's flora. *Natl. Sci. Rev.* **2018**, *5*, 237–254. https://doi.org/10.1093/nsr/nwx041

29. Glasspool, I.J.; Scott, A.C.; Waltham, D.; et al. The impact of fire on the late Paleozoic earth system. *Front. Plant Sci.* **2015**, *6*, 756. https://doi.org/10.3389/fpls.2015.00756

30. Shao, L.Y.; Wang, H.; Yu, X.H.; et al. Paleo-fires and atmospheric oxygen levels in the latest Permian, evidence from maceral compositions of coals in Eastern Yunnan, Southern China. *Acta Geol. Sin.* **2012**, *86*, 949–962. https://doi.org/10.1111/j.1755-6724.2012.00719.x

31. Vajda, V.; McLoughlin, S.; Mays, C.; et al. End-Permian (252 Mya) deforestation, wildfires and flooding—An ancient biotic crisis with lessons for the present. *Earth Planet. Sci. Lett.* **2020**, *529*, 115875. https://doi.org/10.1016/j.epsl.2019.115875

32. Scott, A.C. Observations on the nature and origin of fusain. *Int. J. Coal Geol.* **1989**, *12*, 443–475. https://doi.org/10.1016/0166-5162(89)90061-X

33. Zhao, J.R.; Zheng, B.; Ciais, P.; et al. Global warming amplifies wildfire health burden and reshapes inequality. *Nature* **2025**, *647*, 928–934. https://doi.org/10.1038/s41586-025-09612-9

34. Belcher, C.M; Mander, L.; Rein, G.; et al. Increased fire activity at the Triassic/Jurassic boundary in Greenland due to climate-driven floral change. *Nat. Geosci.* **2010**, *3*, 426–429. https://doi.org/10.1038/ngeo871

35. Shao, L.Y.; Wang, X.T.; Wang, D.D.; et al. Sequence stratigraphy, paleogeography, and coal accumulation regularity of major coal-accumulating periods in China. *Int. J. Coal Sci. Technol.* **2020**, *7*, 240–262. https://doi.org/10.1007/s40789-020-00341-0

36. Scott, A.C.; Glasspool, I.J. Charcoal reflectance as a proxy for the emplacement temperature of pyroclastic flow deposits. *Geology* **2005**, *33*, 589–592. https://doi.org/10.1130/G21474.1

37. Song, Y.; Tian, Y.; Yu, J.X.; et al. Wildfire response to rapid climate change during the Permian-Triassic biotic crisis. *Glob. Planet. Change* **2022**, *215*, 103872. https://doi.org/10.1016/j.gloplacha.2022.103872

38. Baker, S.J. Fossil evidence that increased wildfire activity occurs in tandem with periods of global warming in Earth's past. *Earth-Sci. Rev.* **2022**, *224*, 103871. https://doi.org/10.1016/j.earscirev.2021.103871

39. Yan, Z.M.; Shao, L.Y.; Glasspool, I.J.; et al. Frequent and intense fires in the final coals of the Paleozoic indicate elevated atmospheric oxygen levels at the onset of the End-Permian Mass Extinction Event. *Int. J. Coal Geol.* **2019**, *207*, 75–83. https://doi.org/10.1016/j.coal.2019.03.016

40. Hua, F.H.; Shao, L.Y.; Wang, X.T.; et al. The impact of frequent wildfires during the Permian–Triassic transition, Floral change and terrestrial crisis in southwestern China. *Palaeogeogr. Palaeoclimatol. Palaeoecol.* **2024**, *641*, 112129. https://doi.org/10.1016/j.palaeo.2024.112129

41. Shivanna, M.; Murthy, S.; Gautam, S.; et al. Macroscopic charcoal remains as evidence of wildfire from late Permian Gondwana sediments of India, Further contribution to global fossil charcoal database. *Palaeoworld* **2017**, *26*, 638–649. https://doi.org/10.1016/j.palwor.2017.05.003

42. Olivia, H.; Iain, C.P.; Sandy, P.H. Wildfires on a changing planet. *Nat. Commun.* **2026**, *17*, 1599. https://doi.org/10.1038/s41467-025-68176-4

43. Cai, Y.F.; Zhang, H.; Cao, C.Q.; et al. Wildfires and deforestation during the Permian–Triassic transition in the southern Junggar Basin, Northwest China. *Earth-Sci. Rev.* **2021**, *218*, 103670. https://doi.org/10.1016/j.earscirev.2021.103670

44. Jolly, W.M.; Cochrane, M.A.; Freeborn, P.H.; et al. Climate-induced variations in global wildfire danger from 1979 to 2013. *Nat. Commun.* **2015**, *6*, 7537. https://doi.org/10.1038/ncomms8537

45. Kelly, L.T.; Giljohann, K.M.; Duane, A.; et al. Fire and biodiversity in the Anthropocene. *Science* **2020**, *370*, 6519. https://doi.org/10.1126/science.abb0355

46. Stanley, S.M. Estimates of the magnitudes of major marine mass extinctions in earth history. *Proc. Natl. Acad. Sci. USA* **2016**, *113*, E6325–E6334. https://doi.org/10.1073/pnas.1613094113

47. Sun, Y.D.; Farnsworth, A.; Joachimski, M.M.; et al. Mega El Niño instigated the end-Permian mass extinction. *Science* **2024**, *385*, 1189–1195. https://doi.org/10.1126/science.ado2030

48. Bond, D.P.G.; Grasby, S.E. On the causes of mass extinctions. *Palaeogeogr. Palaeoclimatol. Palaeoecol.* **2017**, *478*, 3–29. https://doi.org/10.1016/j.palaeo.2016.11.005

49. Cribb, A.T.; Bottjer, D.J. Complex marine bioturbation ecosystem engineering behaviors persisted in the wake of the end-Permian mass extinction. *Sci. Rep.* **2020**, *10*, 203. https://doi.org/10.1038/s41598-019-56740-0

50. Fan, J.; Shen, S.Z.; Erwin, D.H.; et al. A high-resolution summary of Cambrian to Early Triassic marine invertebrate biodiversity. *Science* **2020**, *367*, 272–277. https://doi.org/10.1126/science.aax495

51. Xiong, C.H.; Wang, J.S.; Huang, P.; et al. Plant resilience and extinctions through the Permian to Middle Triassic on the North China Block, A multilevel diversity analysis of macrofossil records. *Earth-Sci. Rev.* **2021**, *223*, 103846. https://doi.org/10.1016/j.earscirev.2021.103846

52. Tong, J.N.; Chen, Z.Q.; Huang, Y.F. Reconstruction of ecosystem and biotic recovery following the end-permian mass extinction in South China. *J. Earth Sci.* **2010**, *21*, 167–169. https://doi.org/10.1007/s12583-010-0201-2

53. Huang, C.J.; Tong, J.N.; Hinnov, L.; et al. Did the great dying of life take 700 k.y.? Evidence from global astronomical correlation of the Permian-Triassic boundary interval. *Geology* **2011**, *39*, 779–782. https://doi.org/10.1130/G32126.1

54. Yuan, D.X.; Shen, S.Z.; Henderson, C.M.; et al. Revised conodont-based integrated high-resolution timescale for the Changhsingian Stage and end-Permian extinction interval at the Meis-

han sections, South China. *Lithos* **2014**, *204*, 220–245. https://doi.org/10.1016/j.lithos.2014.03.026

55. Song, H.J.; Wignall, P.B.; Tong, J.N.; et al. Two pulses of extinction during the Permian–Triassic crisis. *Nat. Geosci.* **2012**, *6*, 52–56. https://doi.org/10.1038/ngeo1649
56. Zheng, Q.F.; Cao, C.Q.; Zhang, M.Y. Sedimentary features of the Permian-Triassic boundary sequence of the Meishan section in Changxing County, Zhejiang Province. *Sci. China Earth Sci.* **2013**, *56*, 956–969. https://doi.org/10.1007/s11430-013-4602-9
57. Xie, S.C.; Pancost, R.D.; Huang, J.H.; et al. Changes in the global carbon cycle occurred as two episodes during the Permian–Triassic crisis. *Geology* **2007**, *35*, 1083–1086. https://doi.org/10.1130/G24224A.1
58. Kamo, S.L.; Czamanske, G.K.; Amelin, Y.; et al. Rapid eruption of Siberian flood-volcanic rocks and evidence for coincidence with the Permian–Triassic boundary and mass extinction at 251 Ma. *Earth Planet. Sci. Lett.* **2003**, *214*, 75–91. https://doi.org/10.1016/S0012-821X(03)00347-9
59. Grasby, S.E.; Them, T.R.; Chen, Z.; et al. Mercury as a proxy for volcanic emissions in the geologic record. *Earth-Sci. Rev.* **2019**, *196*, 102880. https://doi.org/10.1016/j.earscirev.2019.102880
60. Shen, J.; Yu, J.X.; Chen, J.B.; et al. Mercury evidence of intense volcanic effects on land during the Permian-Triassic transition. *Geology* **2019**, *47*, 1117–1121. https://doi.org/10.1130/G46679.1
61. Wang, X.D.; Cawood, P.A.; Grasby, S.E.; et al. Characteristics of Hg concentrations and isotopes in terrestrial and marine facies across the end-Permian mass extinction. *Glob. Planet. Change* **2021**, *205*, 103592. https://doi.org/10.1016/j.gloplacha.2021.103592
62. He, B.; Zhong, Y.T.; Xu, Y.G.; et al. Triggers of Permo-Triassic boundary mass extinction in South China, The Siberian Traps or Paleo-Tethys ignimbrite flare-up? *Lithos* **2014**, *204*, 258–267. https://doi.org/10.1016/j.lithos.2014.05.011
63. Wang, J.; Shao, L.Y.; Wang, H.; et al. SHRIMP zircon U–Pb ages from coal beds across the Permian–Triassic boundary, eastern Yunnan, southwestern China. *J. Palaeogeogr.* **2018**, *7*, 117–129. https://doi.org/10.1016/j.jop.2018.01.002
64. Black, B.A.; Lamarque, J.F.; Shields, C.A.; et al. Acid rain and ozone depletion from pulsed Siberian Traps magmatism. *Geology* **2014**, *42*, 67–70. https://doi.org/10.1130/G34875.1
65. Benton, M.J. Hyperthermal-driven mass extinctions, killing models during the Permian-Triassic mass extinction. *Philos. Trans. A Math. Phys. Eng. Sci.* **2018**, *376*, 2130. https://doi.org/10.1098/rsta.2017.0076
66. Cui, Y.; Bercovici, A.; Yu, J.X.; et al. Carbon cycle perturbation expressed in terrestrial Permian–Triassic boundary sections in South China. *Glob. Planet. Change* **2017**, *148*, 272–285. https://doi.org/10.1016/j.gloplacha.2015.10.018
67. Li, M.H.; Frank, T.D.; Xu, Y.L.; et al. Sulfur isotopes link atmospheric sulfate aerosols from the Siberian Traps outgassing to the end-Permian extinction on land. *Earth Planet. Sci. Lett.* **2022**, *592*, 117634. https://doi.org/10.1016/j.epsl.2022.117634
68. Wang, H., Shao, L.Y., Newton, R.J., et al. Records of terrestrial sulfur deposition from the latest Permian coals in SW China. *Chem. Geol.* **2012**, *292–293*, 18–24. https://doi.org/10.1016/j.chemgeo.2011.11.005
69. Chen, B.; Joachimski, M.M.; Shen, S.Z.; et al. Permian ice volume and palaeoclimate history, Oxygen isotope proxies revisited. *Gondwana Res.* **2013**, *24*, 77–89. https://doi.org/10.1016/j.gr.2012.07.007
70. Chen, J.; Shen, S.Z.; Li, X.H.; et al. High-resolution SIMS oxygen isotope analysis on conodont apatite from South China and implications for the end-Permian mass extinction. *Palaeogeogr. Palaeoclimatol. Palaeoecol.* **2016**, *448*, 26–38. https://doi.org/10.1016/j.palaeo.2015.11.025
71. Song, H.J.; Song, H.Y.; Tong, J.N.; et al. Conodont calcium isotopic evidence for multiple shelf acidification events during the early Triassic. *Chem. Geol.* **2021**, *562*, 120038. https://doi.org/10.1016/j.chemgeo.2020.120038
72. Miao, X.; Chu, D.L.; Tong, J.N.; et al. Biostratigraphic significance and geometric morphometrics of Euestheria gutta (Crustacea, Branchiopoda, Spinicaudata), An index fossil of continental Permian–Triassic transitional beds. *Geol. J.* **2021**, *56*, 6176–6188. https://doi.org/10.1002/gj.4096
73. Chu, D.L.; Corso, J.D.; Shu, W.C.; et al. Metal-induced stress in survivor plants following the end-Permian collapse of land ecosystems. *Geology* **2021**, *49*, 657–661. https://doi.org/10.1130/G48333.1
74. Liu, F.; Peng, H.; Marshall, J.E.A.; et al. Dying in the Sun, Direct evidence for elevated UV-B radiation at the end-Permian mass extinction. *Sci. Adv.* **2023**, *9*, eabo6102. https://doi.org/10.1126/ sciadv.abo6102
75. Wu, Y.Y.; Chu, D.L.; Tong, J.N.; et al. Six-fold increase of atmospheric pCO_2 during the Permian–Triassic mass extinction. *Nat. Commun.* **2021**, *12*, 2137. https://doi.org/10.1038/s41467-021-22298-7
76. Garbelli, C.; Angiolini, L.; Shen, S.Z. Biomineralization and global change, A new perspective for understanding the end-Permian extinction. *Geology* **2017**, *45*, 19–22. https://doi.org/10.1130/G38430.1
77. Takahashi, S.; Hori, R.S.; Yamakita, S.; et al. Progressive development of ocean anoxia in the end-Permian pelagic Panthalassa. *Glob. Planet. Change.* **2021**, *207*, 103650. https://doi.org/10.1016/j.gloplacha.2021.103650
78. Ward, P.D.; Botha, J.; Buick, R.; et al. Abrupt and gradual extinction among Late Permian land vertebrates in the Karoo basin, South Africa. *Science* **2005**, *307*, 709–714. https://doi.org/10.1126/ science.1107068
79. Viglietti, P.A.; Benson, R.B.J.; Smith, R.M.H.; et al. Evidence from South Africa for a protracted end-Permian extinction on land. *Proc. Natl. Acad. Sci. USA* **2021**, *118*, e2017045118. https://doi.org/10.1073/pnas.2017045118
80. Fielding, C.R.; Frank, T.D.; Tevyaw, A.P.; et al. Sedimentology of the continental end-Permian extinction event in the Sydney Basin, eastern Australia. *Sedimentology* **2020**, *68*, 30–62. https://doi.org/10.1111/sed.12782
81. Zhang, H.; Cao, C.Q.; Liu, X.L.; et al. The terrestrial end-Permian mass extinction in South China. *Palaeogeogr. Palaeoclimatol. Palaeoecol.* **2016**, *448*, 108–124. https://doi.org/10.1016/j.palaeo.2015.07.002
82. Jurikova, H.; Gutjahr, M.; Wallmann, K.; et al. Permian–Triassic mass extinction pulses driven by major marine carbon cycle perturbations. *Nat. Geosci.* **2020**, *13*, 745–750. https://doi.org/10.1038/s41561-020-00646-4
83. Berner, R.A. Atmospheric carbon dioxide levels over Phanerozoic time. *Science* **1990**, *249*, 1382–1386. https://doi.org/10.1126/ science.249.4975.138
84. Newton, R.; Bottrell, S. Stable isotopes of carbon and sulphur as indicators of environmental change, past and present. *J. Geol. Soc.* **2007**, *164*, 691–708. https://doi.org/10.1144/0016-76492006-101
85. Payne, J.L.; Lehrmann, D.J.; Wei, J.Y.; et al. Large perturbations of the carbon cycle during recovery from the End-Permian extinction. *Science* **2004**, *305*, 506–509. https://doi.org/10.1126/science.1097023
86. Bercovici, A.; Cui, Y.; Forel, M.B.; et al. Terrestrial paleoenvironment characterization across the Permian–Triassic boundary in South China. *J. Asian Earth Sci.* **2015**, *98*, 225–246. https://doi.org/10.1016/j.jseaes.2014.11.016
87. Yu, J.X.; Broutin, J.; Chen, Z.Q.; et al. Vegetation changeover across the Permian–Triassic Boundary in Southwest China. *Earth-Sci. Rev.* **2015**, *149*, 203–224. https://doi.org/10.1016/j.earscirev.2015.04.005
88. Burgess, S.D.; Bowring, S.A. High-precision geochronology confirms voluminous magmatism before, during, and after Earth's most

severe extinction. *Sci. Adv.* **2015**, *1*, e1500470. https://doi.org/10.1126/sciadv.1500470

89. Shen, J.; Chen, J.; Algeo, T.J.; et al. Evidence for a prolonged Permian-Triassic extinction interval from global marine mercury records. *Nat. Commun.* **2019**, *10*, 1563. https://doi.org/10.1038/s41467-019-09620-0
90. Chen, J.B.; Sun, G.Y.; Lu, B.J.; et al. Inconsistent mercury records from terrestrial upland to coastal lowland across the Permian-Triassic transition. *Earth Planet. Sci. Lett.* **2023**, *614*, 118195. https://doi.org/10.1016/j.epsl.2023.118195
91. Wu, Q.; Ramezani, J.; Zhang, H.; et al. High-precision U-Pb age constraints on the Permian floral turnovers, paleoclimate change, and tectonics of the North China block. *Geology* **2021**, *49*, 677–681. https://doi.org/10.1130/G48051.1
92. Xiong, C.H.; Wang, Q. Permian–Triassic land-plant diversity in South China, Was there a mass extinction at the Permian/Triassic boundary? *Paleobiology* **2016**, *37*, 157–167. https://doi.org/10.1666/09029.1
93. Xu, Z.; Hilton, J.; Yu, J.X.; et al. End Permian to Middle Triassic plant species richness and abundance patterns in South China, Coevolution of plants and the environment through the Permian–Triassic transition. *Earth-Sci. Rev.* **2022**, *232*, 104136. https://doi.org/10.1016/j.earscirev.2022.104136
94. Spina, A.; Rettori, G.; Cirilli, S.; et al. Progress of the palynozonation of the middle to late Permian of the Zagros Basin (SW Iran) and Central Iran. *Palaeogeogr. Palaeoclimatol. Palaeoecol.* **2026**, 113982. https://doi.org/10.1016/j.palaeo.2026.113982
95. Rees, P.M. Land-plant diversity and the end-Permian mass extinction. *Geology* **2015**, *30*, 827–830. https://doi.org/10.1130/0091-7613(2002)030<0827
96. Peng, Y.; Shi, G.R. Life crises on land across the Permian–Triassic boundary in South China. *Glob. Planet. Change* **2009**, *65*, 155–165. https://doi.org/10.1016/j.gloplacha.2008.10.016
97. Spina, A.; Cirilli, S.; Utting, J.; et al. Palynology of the Permian and Triassic of the Tesero and Bulla sections (Western Dolomites, Italy) and consideration about the enigmatic species *Reduviasporonites chalastus*. *Rev. Palaeobot. Palynol.* **2015**, *218*, 3–14. https://doi.org/10.1016/j.revpalbo.2014.10.003
98. Rampino, M.R.; Eshet, Y. The fungal and acritarch events as time markers for the latest Permian mass extinction, An update. *Geosci. Front.* **2018**, *9*, 147–154. https://doi.org/10.1016/j.gsf.2017.06.005
99. Hochuli, P.A.; Hermann, E.; Vigran, J.O.; et al. Rapid demise and recovery of plant ecosystems across the end-Permian extinction event. *Glob. Planet. Change* **2010**, *74*, 144–155. https://doi.org/10.1016/j.gloplacha.2010.10.004
100. Bourquin, S.; Rossignol, C.; Jolivet, M.; et al. Reply to the comment on “Terrestrial Permian-Triassic boundary in southern China, New stratigraphic, structural and palaeoenvironment considerations” by H. Zhang, Z. Feng, J. Ramezanik, S-Z Shen. *Palaeogeogr. Palaeoclimatol. Palaeoecol.* **2018**, *506*, 257–259. https://doi.org/10.1016/j.palaeo.2018.02.021
101. Zhang, H.; Feng, Z.; Ramezani, J.; et al. Comments on “Terrestrial Permian–Triassic boundary in southern China, New stratigraphic, structural and palaeoenvironment considerations” by Bourquin et al. (2018). *Palaeogeogr. Palaeoclimatol. Palaeoecol.* **2018**, *506*, 254–256. https://doi.org/10.1016/j.palaeo.2018.02.019
102. Peng, Y.Q.; Yu, J.X.; Gao, Y.Q.; et al. Palynological assemblages of non-marine rocks at the Permian–Triassic boundary, western Guizhou and eastern Yunnan, South China. *J. Asian Earth Sci.* **2006**, *28*, 291–305. https://doi.org/10.1016/j.jseaes.2005.10.007
103. DiMichele, W.A.; Bashforth, A.R.; Falcon-Lang, H.J.; et al. Uplands, lowlands, and climate, Taphonomic megabiases and the apparent rise of a xeromorphic, drought-tolerant flora during the Pennsylvanian-Permian transition. *Palaeogeogr. Palaeoclimatol. Palaeoecol.* **2020**, *559*, 109965. https://doi.org/10.1016/j.palaeo.2020.109965
104. Nowak, H.; Schneebeli-Hermann, E.; Kustatscher, E. No mass extinction for land plants at the Permian-Triassic transition. *Nat. Commun.* **2019**, *10*, 384. https://doi.org/10.1038/s41467-018-07945-w
105. Zhang, P.X.; Yang, M.F.; Lu, J.; et al. End-Permian terrestrial ecosystem collapse in North China, Evidence from palynology and geochemistry. *Glob. Planet. Change* **2023**, *222*, 104070. https://doi.org/10.1016/j.gloplacha.2023.104070
106. Ouyang, S.; Hou, J.P. On characteristics of the Cathaysian Palynoflora. *Acta Palaeontol. Sin.* **1999**, *38*, 261–283. https://doi.org/10.3969/j.issn.0001-6616.1999.03.001
107. Broutin, J.; Yu, J.X.; Shi, X.; et al. Terrestrial palaeofloral succession across the Permian–Triassic Boundary in the North and South China blocks, a brief review. *PalZ* **2020**, *94*, 633–644. https://doi.org/10.1007/s12542-020-00511-0
108. Guo, W.W.; Tong, J.N.; He, Q.; et al. Late Permian–Middle Triassic magnetostratigraphy in North China and its implications for terrestrial-marine correlations. *Earth Planet. Sci. Lett.* **2022**, *585*, 117519. https://doi.org/10.1016/j.epsl.2022.117519
109. Nowak, H.; Vérard, C.; Kustatscher, E. Palaeophytogeographical patterns across the Permian–Triassic boundary. *Front. Earth Sci.* **2020**, *8*, 613350. https://doi.org/10.3389/feart.2020.613350
110. Li, M.S.; Ogg, J.; Zhang, Y.; et al. Astronomical tuning of the end-Permian extinction and the Early Triassic Epoch of South China and Germany. *Earth Planet. Sci. Lett.* **2016**, *441*, 10–25. https://doi.org/10.1016/j.epsl.2016.02.017
111. Su, C.M.; Chen, Z.Q.; Wang, X.; et al. Biotic and palaeoecological variations in the Permian-Triassic boundary microbialite (Xiejiacao, South China), Implication for a two-phase ecological crisis in microbialite ecosystems. *Glob. Planet. Change* **2021**, *207*, 103679. https://doi.org/10.1016/j.gloplacha.2021.103679
112. Aftabuzzaman, M.; Kaiho, K.; Biswas, R.K.; et al. End-Permian terrestrial disturbance followed by the complete plant devastation, and the vegetation proto-recovery in the earliest-Triassic recorded in coastal sea sediments. *Glob. Planet. Change* **2021**, *205*, 103621. https://doi.org/10.1016/j.gloplacha.2021.103621
113. Wu, J.Q.; Chu, D.L.; Luo, G.M.; et al. Stepwise deforestation during the Permian-Triassic boundary crisis linked to rising temperatures. *Earth Planet. Sci. Lett.* **2023**, *620*, 118350. https://doi.org/10.1016/j.epsl.2023.118350
114. Ruprecht, J.K.; Schofield, N.J. Effects of partial deforestation on hydrology and salinity in high salt storage landscapes. II. Strip, soils and parkland clearing. *J. Hydrol.* **1991**, *129*, 19–38. https://doi.org/10.1016/0022-1694(91)90042-G
115. Feng, Z.; Wei, H.B.; Ye, R.H.; et al. Latest Permian peltasperm plant from southwest china and its paleoenvironmental implications. *Front. Earth Sci.* **2020**, *8*, 559430. https://doi.org/10.3389/feart.2020.559430
116. Schneebeli-Hermann, E.; Hochuli, P.A.; Bucher, H. Palynofloral associations before and after the Permian–Triassic mass extinction, Kap Stosch, East Greenland. *Glob. Planet. Change* **2017**, *155*, 178–195. https://doi.org/10.1016/j.gloplacha.2017.06.009
117. Kaiho, K.; Yatsu, S.; Oba, M.; et al. A forest fire and soil erosion event during the Late Devonian mass extinction. *Palaeogeogr. Palaeoclimatol. Palaeoecol.* **2013**, *392*, 272–280. https://doi.org/10.1016/j.palaeo.2013.09.008
118. Lee, J.S.; Cornwell, W.K.; Kingsford, R.T. Rainforest bird communities threatened by extreme fire. *Glob. Ecol. Conserv.* **2022**, *33*, e01985. https://doi.org/10.1016/j.gecco.2021.e01985
119. Mays, C.; McLoughlin, S. End-Permian Burnout, the role of Permian–Triassic wildfires in extinction, carbon cycling, and environmental change in Eastern Gondwana. *Palaios* **2022**, *37*, 292–317. https://doi.org/10.2110/palo.2021.051
120. Cao, C.Q.; Wang, W.; Liu, L.J.; et al. Two episodes of 13C-depletion in organic carbon in the latest Permian, Evidence from the terrestrial sequences in northern Xinjiang, China. *Earth Planet. Sci. Lett.* **2008**, *270*, 251–257. https://doi.org/10.1016/j.epsl.2008.03.043

121. Zhou, W.F.; Algeo, T.J.; Luo, G.M.; et al. Hydrocarbon compound evidence in marine successions of South China for frequent wildfires during the Permian-Triassic transition. *Glob. Planet. Change* **2021**, *200*, 103472. https://doi.org/10.1016/j.gloplacha.2021.103472

122. Richardson, D.; Black, A.S.; Irving, D.; et al. Global increase in wildfire potential from compound fire weather and drought. *npj Clim. Atmos. Sci.* **2022**, *5*, 23. https://doi.org/10.1038/s41612-022-00248-4

123. Jiao, S.L.; Zhang, H.; Cai, Y.F.; et al. Collapse of tropical rainforest ecosystems caused by high-temperature wildfires during the end-Permian mass extinction. *Earth Planet. Sci. Lett.* **2023**, *614*, 118193. https://doi.org/10.1016/j.epsl.2023.118193

124. Glasspool, I.J.; Scott, A.C. Phanerozoic concentrations of atmospheric oxygen reconstructed from sedimentary charcoal. *Nat. Geosci.* **2010**, *3*, 627–630. https://doi.org/10.1038/ngeo923

125. Wang, Y.; Lu, J.; Yang, M.F.; et al. Volcanism and wildfire associated with deep-time deglaciation during the Artinskian (early Permian). *Glob. Planet. Change* **2023**, *225*, 104126. https://doi.org/10.1016/j.gloplacha.2023.104126

126. Krause, A.J.; Mills, B.J.W.; Zhang, S.; et al. Stepwise oxygenation of the Paleozoic atmosphere. *Nat. Commun.* **2018**, *9*, 4081. https://doi.org/10.1038/s41467-018-06383-y

127. Nascimento, M.N.; Heijink, B.M.; Bush, M.B.; et al. Early to mid-Holocene human activity exerted gradual influences on Amazonian forest vegetation. *Philos. Trans. R. Soc. Lond. B Biol. Sci.* **2022**, *377*, 20200498. https://doi.org/10.1098/rstb.2020.0498

128. Riel, N.; Jaillard, E.; Martelat, J.E.; et al. Permian-Triassic Tethyan realm reorganization, Implications for the outward Pangea margin. *J. S. Am. Earth Sci.* **2018**, *81*, 78–86. https://doi.org/10.1016/j.jsames.2017.11.007

129. Feng, X.; Merow, C.; Liu, Z.; et al. How deregulation, drought and increasing fire impact Amazonian biodiversity. *Nature* **2021**, *597*, 516–521. https://doi.org/10.1038/s41586-021-03876-7

130. Staver, A.C.; Archibald, S.; Levin, S.A. The global extent and determinants of Savanna and Forest as alternative biome states. *Science* **2011**, *334*, 230–232. https://doi.org/10.1126/science.1210465

131. Clarke, P.J.; Prior, L.D.; French, B.J.; et al. Using a rainforest-flame forest mosaic to test the hypothesis that leaf and litter fuel flammability is under natural selection. *Oecologia* **2014**, *176*, 1123–1133. https://doi.org/10.1007/s00442-014-3071-y

132. Cochrane, M.A. Fire science for rainforests. *Nature* **2022**, *421*, 913–919. https://doi.org/10.1038/nature01437

133. Li, S.H.; Ethan, L.G.; Zhang, S.; et al. Erosion-driven delayed warming and marine stress prior to the end-Permian mass extinction. *Nat. Commun.* **2026**, *17*, 5456. https://doi.org/10.1038/s41467-026-74636-2

134. Wang, W.Q.; Garbelli, C.; Zhang, F.F.; et al. A high-resolution Middle to Late Permian paleotemperature curve reconstructed using oxygen isotopes of well-preserved brachiopod shells. *Earth Planet. Sci. Lett.* **2020**, *540*, 116245. https://doi.org/10.1016/j.epsl.2020.116245

135. Cui, Y.; Li, M.; Van Soelen, E.E.; et al. Massive and rapid predominantly volcanic CO_2 emission during the end-Permian mass extinction. *Proc. Natl. Acad. Sci. USA* **2021**, *118*, e2014701118. https://doi.org/10.1073/pnas.2014701118

136. Wu, Y.Y.; Cui, Y.; Chu, D.L.; et al. Volcanic CO_2 degassing postdates thermogenic carbon emission during the end-Permian mass extinction. *Sci. Adv.* **2023**, *9*, eabq4082. https://doi.org/10.1126/sciadv.abq4082

137. Cai, Y.F.; Zhang, H.; Feng, Z.; et al. Intensive wildfire associated with volcanism promoted the vegetation changeover in Southwest China during the permian–triassic transition. *Front. Earth Sci.* **2021**, *9*, 615841. https://doi.org/10.3389/feart.2021.615841